Estimating Dynamic Spillover Effects along Multiple Networks in a Linear Panel Model

Clemens Possnig[1], Andreea Rotărescu[2], and Kyungchul Song[3]

September 7, 2022

Abstract. Spillover of economic outcomes often arises over multiple networks, and distinguishing their separate roles is important in empirical research. For example, the direction of spillover between two groups (such as banks and industrial sectors linked in a bipartite graph) has important economic implications, and a researcher may want to learn which direction appears prominent in data. For this, we need to have an empirical methodology that allows for both directions of spillover simultaneously. In this paper, we develop a dynamic linear panel model and asymptotic inference with large n and small T, where both directions of spillover are accommodated through multiple networks. Using the methodology developed here, we perform an empirical study of spillovers between bank weakness and zombie-firm congestion in industrial sectors, using firm-bank matched data from Spain between 2005 and 2012. Overall, we find that there is positive spillover in both directions between banks and sectors.

Key words. Spillover Effects; Networks; Fixed Effects; Dynamic Linear Panel Models; Cross-Sectional Dependence; Sector-Bank Spillover; Zombie Lending; Capital Misallocation

JEL Classification: C12, C21, C31, E44, G21, G32

[1]Vancouver School of Economics, University of British Columbia
[2]Department of Economics, Johns Hopkins University
[3]Vancouver School of Economics, University of British Columbia
Date: September 7, 2022.
All errors are ours. Song acknowledges that this research was supported by Social Sciences and Humanities Research Council of Canada. Corresponding address: Kyungchul Song, Vancouver School of Economics, University of British Columbia, 6000 Iona Drive, Vancouver, BC, V6T 1L4, Canada. Email address: kysong@mail.ubc.ca.

1. Introduction

Many economic outcomes, such as profits of firms or performance of students, evolve over time, producing spillover effects on other units over multiple large networks. Each network captures a distinct aspect of the relationship between units, and serves as a channel of spillover effects between them. A researcher may want to investigate statistical significance of spillover effects separately for each network. One prominent example is a setting with two directed bipartite networks between two groups of cross-sectional units, where one network represents a channel of spillover from one group to the other, and the other network represents its opposite direction. A researcher may want to see which direction of spillover is empirically supported. For this, she needs to find an empirical methodology that allows for both directions of spillovers simultaneously.

Our paper is motivated by one important area of empirical research which concerns the spillover that arises between banks and firms.[1] Banks and firms are naturally interconnected through their lending relationships and as such heavily influence one another. Bank health, for one, can be a powerful determinant of firm performance. For example, banks with weak balance sheets may cut lending to their borrowers, thereby depriving them of the funds they need to operate and to invest. Firm performance, in turn, can act as an important driver of bank health: when firms miss payments on their loans, the banks issuing those loans suffer losses which put them in a worse financial position. In this setting, establishing which direction of outcome propagation is significant has important policy implications. If the direction pointing from the banking sector to the real sector is significant, then this makes the case for having prudential regulation in place which ensures that banks are well capitalized and able to absorb shocks to their balance sheets. If, additionally, the spillover from the real sector to the banking sector is significant, then policies that foster a more dynamic business environment might prove beneficial. This includes making it easier for incumbent firms to adjust the scale of their activity, as well as facilitating the exit of inefficient firms. These goals could be achieved, for example, by reducing factor adjustment costs and reforming insolvency regimes.

In this paper, we focus on a dynamic linear panel model where the spillover effects are captured by averages of past outcomes of neighbors across network measurements. For the empirical applications we have in mind, the spillover effects along a network are often detected through the correlation between outcomes in one period and their neighbors' outcomes in the previous period, after controlling for covariates. However, such correlation can arise

[1]There is a large and growing empirical literature exploring the real economic effects of bank distress. See, for example, Peek and Rosengren (2000), Khwaja and Mian (2008) and Chodorow-Reich (2014) for seminal contributions.

simply through time effects that are specific to the cluster that those outcomes commonly belong to. For example, the outcomes of two firms can be correlated because they belong to the same industrial sector and there have been industry specific demand shocks over time. This correlation between the firms has nothing to do with spillover effects between firms along a network, and yet contributes to the spillover effects measured through such correlations. To separate out cross-sectional correlation due to cluster-specific time effects, we include cluster-specific time effects and define the spillover effect to be one that is due to the spatio-temporal variations of outcomes *net of* cluster-specific time averages of the outcomes.

Employing the Helmert transform of Arellano and Bover (1995), we develop an estimation procedure of the parameters, and asymptotic inference on those parameters. Our method of estimation and inference is simple, and does not involve any numerical optimization. We also propose a simple multiple testing procedure to detect the direction of spillover effect between two groups while controlling for the familywise error rate (FWER) asymptotically. From an extensive Monte Carlo simulation study, we find that the asymptotic inference performs very well, over a wide range of network configurations.

Using the methodology developed in this paper, we perform an empirical study of spillover between banks and industrial sectors using data from Spain. One of the most striking manifestations of the close interdependence between banks and firms is the existence of so-called zombie firms. These are firms which are known to be in financial distress but are artificially kept alive by weak banks seeking to avoid, or at least postpone, further damaging their balance sheets by realizing the losses caused by these firms. The practice of extending credit to zombie firms, also known as loan evergreening, was first documented in the context of Japan's "lost decade" and has attracted renewed attention in light of the weak economic recovery in Europe following the global financial crisis and the subsequent sovereign debt crisis.[2]

Keeping zombie firms afloat can have adverse spillover effects on the rest of the economy by inhibiting the movement of resources from less productive to more productive uses. Indeed, a number of recent studies provide evidence linking an increase in zombie-firm congestion to

[2]For early evidence from Japan, see Peek and Rosengren (2005), Caballero, Hoshi, and Kashyap (2008) and Giannetti and Simonov (2013). For more recent evidence from Europe, see Acharya, Eisert, Eufinger, and Hirsch (2019), Blattner, Farinha, and Rebelo (2019) and Schivardi, Sette, and Tabellini (2022). For a recent survey of the theoretical and empirical literature on zombie lending, see Acharya, Crosignani, Eisert, and Steffen (2022).

a deterioration in sector-level competition, innovation, and productivity-enhancing reallocation.[3] These findings are particularly worrisome, given that sclerotic business environments with a high degree of resource misallocation have been shown to contribute to sizable losses in aggregate productivity.[4]

Motivated by this discussion, we choose to focus our empirical application on the relationship between bank health and zombie-firm congestion in narrow sectors of activity. Our application is thematically related to a large body of research on the real effects of the bank lending channel, however, we depart from this literature in important methodological ways. Much of the literature has focused on one direction in the causal link, namely the one originating from banks. A common approach in this literature has been to identify exogenous shocks to bank health and trace their effect on bank lending and various types of real economic activity.[5] What makes such an approach challenging is the possibility that, regardless of one's definition of a fragile bank, the composition of the bank's borrower pool contributed to that fragility.

Our framework allows us to take a more general approach which differs from the previous empirical literature in two crucial ways. First, we are able to separately measure both directions of spillover – from sectors to banks and from banks to sectors – and to determine whether the effect is significant in either or both directions. Second, our analysis is not contingent on a singular source of exogenous variation, such as a crisis or an unexpected policy announcement. To our knowledge, ours is the first empirical application to jointly estimate *both* directions of outcome spillover between the banking sector and the real sector and take a stand on their joint significance.

We use firm-bank matched data from Spain between 2005 and 2012 to construct a measure of zombie congestion at the 3-digit sector level based on firms' interest coverage ratios and a measure of bank weakness based on reported loan loss provisions. Using directed networks, which capture the dependence between banks and sectors, we implement our estimator and test for the presence of spillover effects between zombie-firm congestion and bank fragility along these networks. We find sizable and significant positive spillover in both directions: a

[3]For example, Acharya, Eisert, Eufinger, and Hirsch (2019) document a reduction in employment growth and investment of non-zombie firms in industries with a high presence of zombie firms in the euro area. Adalet McGowan, Andrews, and Millot (2018) additionally find high zombie congestion to be linked with less productivity-enhancing capital reallocation in an international cross-country sample. Schmidt, Schneider, Steffen, and Streitz (2020) present evidence from Spain which shows capital misallocation from zombie lending to adversely impact output, competition, and patent applications.

[4]See Hsieh and Klenow (2009) and, more recently, Gopinath, Kalemli-Ozcan, Karabarbounis, and Villegas-Sanchez (2017).

[5]For example, Peek and Rosengren (2000), Khwaja and Mian (2008), Chodorow-Reich (2014), Bentolila, Jansen, and Jiménez (2018) provide evidence that a decline in bank health can cause banks to contract lending, raise rates, and/or have an impact on foreign markets or employment.

one standard deviation increase in the sector-level zombie share increases banks' loan loss provisions ratio by about 8.7 p.p. thereby weakening their balance sheets. At the same time, weaker banks lead to an increase in the prevalence of zombie firms: an increase of 8.7 p.p. of the loan loss provision ratio leads to a 1.2 p.p. increase in the share of a sector's assets that are sunk in zombie firms.

Our results imply that bank fragility and inefficient resource allocation, as proxied by the degree of zombie congestion, feed into and reinforce each other. From a policy perspective, this means that a combination of prudential bank regulation and policies fostering a dynamic business environment is needed to avoid aggregate productivity losses.

Literature Review

The literature of dynamic linear panel models with large n and small T has developed various ways to accommodate fixed effects by transforming the linear models. (See Chamberlain (1984) and Arellano and Honoré (2001) for an overview of this literature.) Our method relies on the transform suggested by Arellano and Bover (1995). See Hayakawa (2009) for a related study of efficient instrumental variables. Our cluster-specific time effects can be viewed as a special case of interactive effects, where we impose equality among the factor loadings in the same cluster. See Holtz-Eakin, Newey, and Rosen (1988) and Ahn, Lee, and Schmidt (2001), and more recently, Kuersteiner and Prucha (2020). The literature of linear panel models with interactive effects has also developed asymptotic theory with large n and large T. (See Fernandez-Val and Weidner (2018) for a review of the related literature. See also Shi and Lee (2017) for a spatial dynamic panel model with interactive effects.)

Econometric models that allow for spillover effects over cross-sectional units and cross-sectional dependence have been developed in the literature. (The literature is vast. We refer the reader to Lee (2004), Lee and Yu (2010), Lee, Liu, and Lin (2010), Kuersteiner and Prucha (2013) and Kuersteiner and Prucha (2020) and references therein.) The perspective of spillover effects realizing along multiple networks has received attention in the literature. Egami (2021) developed methods sensitivity analysis when there are unobserved networks that capture part of the spillover effects. Drukker, Egger, and Prucha (2022) proposed asymptotic analysis of estimation and inference procedures in a linear spatial model, which accommodates multiple networks.

To the best of our knowledge, the proposal of Kuersteiner and Prucha (2020) covers the most general class of linear panel models accommodating interactive effects, lagged dependent variables and spatial dependence both in the explanatory variables and errors within the large n and small T framework. They proposed a generalized version of the Helmert transform in Arellano and Bover (1995), and developed asymptotic theory as $n \to \infty$ while T is fixed. While the main focus of Kuersteiner and Prucha (2020) was to develop general

asymptotic inference that covers a wide range of linear panel models, our paper pursues a more parsimonious model which is motivated by an area of empirical research on spillover along multiple networks, where each network carries distinct economic interpretation as a channel of causal effects among cross-sectional units. As such, the estimation and inference procedures and the techniques used for the development of asymptotic theory are different from those of Kuersteiner and Prucha (2020).

Our paper is organized as follows. In the next section, we present a linear panel model of spillover along multiple large networks. We also demonstrate how this model can be extended to accommodate the spillover effects between two groups of cross-sectional units. In Section 3, we introduce the estimation and inference procedures, and provide conditions under which the procedures are asymptotically valid. We also develop the method of inference on the direction of spillovers using a multiple testing procedure and show that it controls FWER asymptotically. In this section, we present results from our Monte Carlo simulation study which show that the inference procedures perform reasonably well across a wide class of network structures. In Section 4, we apply our methods to the empirical analysis of spillover effects between firms and banks in Spain. In Section 5, we conclude. The mathematical proofs of the asymptotic inference results and further results on Monte Carlo simulations and empirical study in this paper are found in the Online Appendix.

2. Spillover along Multiple Large Networks

2.1. A Linear Panel Model of Spillover along Networks

Let us first present a dynamic linear panel model that can be useful to study the spillover of outcomes over multiple large networks. Later we extend our model to one that enables us to study the direction of spillover effects between two groups of cross-sectional units. We assume that there are L observed large networks over a set N of cross-sectional units, where each network evolves over time. Each cross-sectional unit may represent a person, a household, or a firm, depending on the application. The networks may represent friendship among people or business relations among firms. There are multiple networks capturing such relations, where each network captures a distinct aspect of the relationships, but the researcher does not know along which set of networks the spillover effects realize.[6] For each

[6]This lack of knowledge leads to ambiguity about the networks. Estimating the spillover effects with no or partial knowledge of the network structure has received attention in the literature of statistics and econometrics. For example, see Choi (2017), de Paula, Rasul, and Souza (2020), Zhang (2020), Lewbel, Qu, and Tang (2021), and He and Song (2022). Our paper takes a somewhat different perspective; we view that the networks are not necessarily multiple proxy measurements of a single underlying network. Instead, each network reflects a distinct aspect of the relationship between cross-sectional units.

unit i, we denote $N_{t,\ell}(i)$ to represent the in-neighborhood of unit i in the ℓ-th network in time t. That is, the set $N_{t,\ell}(i)$ represents the set of units j whose outcome influences the outcome of unit i. We assume that $i \notin N_{t,\ell}(i)$ for each i and ℓ, so that each unit is not its own neighbor.

Separately from the spillover effect through the networks, each unit i belongs to a cluster and is subject to time-varying cluster-specific common shocks. For example, the correlation between two firms' performance may come from network effects due to their direct interdependence, or just from sector specific macroeconomic common shocks which affect the outcomes of all the firms in the sector. It is important to distinguish between the network effects and sector-specific, time-varying common shocks.

For each cross-sectional unit i, the cluster index is given by $\mu(i) \in \{1, ..., G\}$, so that the equality $\mu(i) = g$ indicates that the unit i belongs to cluster g. Similarly as in the network notation, we denote the set of units in the cluster s by:

$$N_G(i) = \{j \in N : \mu(i) = \mu(j)\}. \tag{2.1}$$

(The subscript G in $N_G(i)$ is mnemonic for "group".) Throughout this paper, we regard the networks as random but the cluster structure as non-random.[7]

Suppose that there is a random variable $y_{i,t}$ representing a continuous outcome for cross-sectional unit i in time t. We define

$$y^G_{i,t} = \frac{1}{|N_G(i)|} \sum_{j \in N_G(i)} y_{j,t}, \tag{2.2}$$

which is the cluster average of outcomes. We assume that $y_{i,t}$'s are generated as follows:

$$y_{i,t} = \alpha_0 y_{i,t-1} + \overline{Y}^\top_{i,t-1}\beta_0 + X^\top_{i,t}\gamma_0 + u_{i,t},$$

where

$$\overline{y}_{i,t-1,\ell} = \frac{1}{|N_{t,\ell}(i)|} \sum_{j \in N_{t,\ell}(i)} (y_{j,t-1} - y^G_{j,t-1}), \tag{2.3}$$

and $\overline{Y}_{i,t-1} = [\overline{y}_{i,t-1,1}, ..., \overline{y}_{i,t-1,L}]^\top$, and $u_{i,t}$ are error terms. (The summation over $N_{t,\ell}(i)$ is taken to be zero, if $N_{t,\ell}(i)$ is empty.) Hence $\overline{y}_{i,t-1,\ell}$ is the average of the previous period mean-deviated outcomes of unit i's neighbors according to the ℓ-th network. The mean deviation is taken to ensure that the parameter β_0 correctly captures the network effect, after controlling for cluster-specific time effects. We will explain this below. It is worth noting that the covariate vector, $X_{i,t}$, can contain lagged covariates.

[7] We assume a time-invariant cluster structure only for the sake of simplicity. Our framework allows for the case where the cluster structure is time-varying so that $g_t(i) = s$ represents that unit i belongs to cluster s in time t, by modifying the definition of filtration appropriately. The estimation and inference procedures remain the same.

We assume that the error term $u_{i,t}$ is decomposed as follows:

$$u_{i,t} = \nu_i + f_{i,t} + \varepsilon_{i,t}, \tag{2.4}$$

where

$$f_{i,t} = \sum_{g=1}^{G} 1\{\mu(i) = g\}\pi_{t,g}. \tag{2.5}$$

The error term (2.4) consists of three components: ν_i, $f_{i,t}$ and $\varepsilon_{i,t}$. The first component ν_i represents time-invariant fixed effects. The term $\varepsilon_{i,t}$ represents unobserved idiosyncratic effects which are independent across cross-sectional units and time, conditional on the past values of other random variables and $X_{i,t}$'s and networks. (We will make clear this conditioning on the past values.) The term $f_{i,t}$ represents *cluster-specific time effects*. For example, each cluster represents an industry sector and $\pi_{t,g}$ captures sector-specific common shocks which are time varying.

In many applications, the main parameter of interest is β_0. The ℓ-th entry of the parameter vector β_0 captures the spillover effect along the ℓ-th network. The model is useful especially when the researcher does not know which network plays a major role in the spillover of outcomes. The model, once properly extended, is also useful when she is interested in exploring the direction of influence between two groups of cross-sectional units. We will demonstrate this in our empirical application.

The substraction of $y^G_{i,t-1}$ in (2.3) distinguishes our model from existing models in the literature, and requires explanation. The subtraction is made to remove any cumulative cluster-specific time effects contained in neighbors' outcomes. First, let us write

$$\frac{1}{|N_{t,\ell}(i)|}\sum_{j\in N_{t,\ell}(i)} y_{j,t-1} = \frac{1}{|N_{t,\ell}(i)|}\sum_{j\in N_{t,\ell}(i)} (y_{j,t-1} - y^G_{i,t-1}) + \frac{1}{|N_{t,\ell}(i)|}\sum_{j\in N_{t,\ell}(i)} y^G_{i,t-1}.$$

When $N_{t,\ell}(i) \neq \varnothing$ for all $i \in N$, the last term is essentially equal to $y^G_{i,t-1}$ which can be absorbed into the cluster time effect $f_{i,t}$. However, when there are isolated nodes, the last term cannot be absorbed into the cluster-specific time effects $\pi_{t,g}$, and has a cross-sectional variation within the same cluster, because it is the same as

$$y^G_{i,t-1} 1\{N_{t,\ell}(i) \neq \varnothing\},$$

which varies if some units in the same cluster are isolated and others are not. However, this variation has nothing to do with the neighbors' outcomes. Hence without subtracting cluster-means, the coefficient β would capture not only the effect of variations in the neighbor's average actions but also variations in the nonemptiness of neighborhoods, which makes it

hard to interpret β as a measure of spillover effect along the networks. Therefore, we consider the form with subtracting $y^G_{i,t-1}$.[8]

In contrast to the outcome generation, we consider a generic model of evolution of networks over time. First, define for each $i \in N$ and t,

$$V_{i,t-1} = \left[y_{i,t-1}, X^\top_{i,t-1}, v_i, f_{i,t-1}, \varepsilon_{i,t-1} \right]^\top. \tag{2.6}$$

Let $\mathcal{V}$ be the space from which $V_{i,t-1}$ takes values. For the network $G_{t,\ell}$, we assume that the link from j to i is formed if and only if $D_{ij,t,\ell} = 1$, where

$$D_{ij,t,\ell} = \varphi_{t,\ell}\left(V_{i,t-1}, V_{j,t-1}\right),$$

where $\varphi_{t,\ell} : \mathcal{V} \times \mathcal{V} \to \{0,1\}$ is a nonstochastic, time varying map. Therefore, the network is formed based on the fixed effects and all the previous period variables that are observed or unobserved. For example, our model accommodates the situation where a firm to bank relation is revised in every period, based on their previous period's performance. Throughout the paper, we do not make a further specification of the functional form of $\varphi_{t,\ell}$ other than noting that it needs to generate sparse enough networks so that our asymptotic theory works.

2.2. Extension: Direction of Spillover Between Banks and Firms

Let us explain how our model can be extended to study the direction of spillovers between two groups of cross-sectional units. First, suppose that the set of cross-sectional units N is divided into two groups

$$N = N_B \cup N_F, \tag{2.7}$$

where we call N_B the set of "banks" and N_F the set of "firms". Again, we assume that a bank and a firm cannot be in the same cluster, that is, the cluster structure is a refinement of the partition (2.7).

At each time t, each node i is associated with an outcome variable $y_{i,t}$. As before, the causal relationship between the variables at each time t is expressed by a set of observed, directed networks whose neighborhoods of a unit i are written as $N_{t,\ell}(i)$, $\ell = 1, ..., L$. For each node i which is either a bank or a firm, we define two in-neighborhoods, one consisting of banks and the other consisting of firms:

$$N_{t,\ell,B}(i) = \{j \in N_B \cap N_G(i) : j \in N_{t,\ell}(i)\}, \text{ and}$$
$$N_{t,\ell,F}(i) = \{j \in N_F \cap N_G(i) : j \in N_{t,\ell}(i)\}.$$

[8] The mean deviation form is still required even if we focus on a single cluster setting, i.e., including only time effects. In this case, we need to consider subtracting the time average of the outcomes.

Hence the set $N_{t,\ell,B}(i)$ denotes the set of banks in $N_G(i)$ whose outcome at time $t-1$ potentially influences the outcome at time t of node i according to network ℓ, and similarly, the set $N_{t,\ell,F}(i)$ the set of firms in $N_G(i)$ whose outcome at time $t-1$ potentially influences the outcome at time t of node i according to the ℓ-th network.

Our primary interest is in the direction of spillover effects between the outcomes of banks and those of firms. To investigate this, let us consider the following linear model. For each $i \in N$, we specify the outcomes to be generated as follows:

$$y_{i,t} = \begin{cases} y_{i,t-1}\alpha_B + \overline{Y}_{i,t-1,B}^{\top}\beta_{BB} + \overline{Y}_{i,t-1,F}^{\top}\beta_{FB} + X_{i,t}^{\top}\gamma_B + u_{i,t}, & \text{if } i \in N_B, \\ y_{i,t-1}\alpha_F + \overline{Y}_{i,t-1,B}^{\top}\beta_{BF} + \overline{Y}_{i,t-1,F}^{\top}\beta_{FF} + X_{i,t}^{\top}\gamma_F + u_{i,t}, & \text{if } i \in N_F, \end{cases} \tag{2.8}$$

where $\overline{Y}_{i,t-1,B} = [\overline{y}_{i,t-1,1,B}, ..., \overline{y}_{i,t-1,L,B}]^{\top}$, and $\overline{Y}_{i,t-1,F} = [\overline{y}_{i,t-1,1,F}, ..., \overline{y}_{i,t-1,L,F}]^{\top}$,

$$\overline{y}_{i,t-1,\ell,B} = \frac{1}{|N_{t,\ell,B}(i)|} \sum_{j \in N_{t,\ell,B}(i)} (y_{j,t-1} - y^G_{j,t-1}), \text{ and}$$

$$\overline{y}_{i,t-1,\ell,F} = \frac{1}{|N_{t,\ell,F}(i)|} \sum_{j \in N_{t,\ell,F}(i)} (y_{j,t-1} - y^G_{j,t-1}).$$

Here we specify $u_{i,t}$ as in (2.4). The parameter β_{BF} captures the impact of the average outcomes of the banks linked to a firm at time $t-1$ on the firm's outcome at time t, similarly β_{FB} that of the average outcomes of the firms linked to a bank at time $t-1$ on the bank's outcome. By computing the joint confidence region for (β_{BF}, β_{FB}), we can check whether the spillover works in only one direction and if so, which direction. In a later section, we provide details on this procedure. We apply this procedure to the investigation of the relation between firms and banks in Spain in our empirical application.

It is important to note that the outcomes do not need be of the "same type" between banks and firms. This flexibility is crucial when analyzing firms and banks because these are very different types of entities and important characteristics defining one group are not well defined for the other. For example, for banks, we can take $y_{i,t}$ to be bank health, as measured by loan loss provisions – a variable which has no natural counterpart on the firm side – whereas for firms, we can take $y_{i,t}$ to be firm health, as measured by the firm's zombie status – a concept which solely applies to firms. In this case, the parameter β_{BF} captures the spillover effect from the previous period's bank health on the health of its linked firms, where "health" has a different meaning for firms than it does for banks.[9]

[9]Productivity is another prominent example of a concept which is only applicable to firms and which is highly related to bank performance. Our framework can accommodate analyzing the spillover between the health of the banking system and firm productivity and hence shed light on aggregate productivity dynamics.

3. Estimation and Inference

3.1. Estimation and Inference

In this section, we focus on the extension in Section 2.2 and explain the estimation and inference procedure. First, we write the dynamic panel model compactly as

$$y_{i,t} = W_{i,t}^{\top}\delta_i + u_{i,t}, \tag{3.1}$$

where $W_{i,t} = [y_{i,t-1}, \overline{Y}_{i,t-1,B}^{\top}, \overline{Y}_{i,t-1,F}^{\top}, X_{i,t}^{\top}]^{\top}$, and

$$\delta_i = \begin{cases} \delta_B \equiv [\alpha_B, \beta_{BB}^{\top}, \beta_{FB}^{\top}, \gamma_B^{\top}]^{\top}, & \text{if } i \in N_B \\ \\ \delta_F \equiv [\alpha_F, \beta_{BF}^{\top}, \beta_{FF}^{\top}, \gamma_F^{\top}]^{\top}. & \text{if } i \in N_F. \end{cases}$$

Hence the parameter vector δ_i takes a different value depending on whether the unit i is a bank or a firm. We construct an estimator of $\delta \equiv [\delta_B^{\top}, \delta_F^{\top}]^{\top}$ using subgroup units as follows.

First, we define cluster-specific averages:

$$Y_{i,t}^{G} = \frac{1}{|N_G(i)|}\sum_{j\in N_G(i)} y_{j,t},\ W_{i,t}^{G} = \frac{1}{|N_G(i)|}\sum_{j\in N_G(i)} W_{j,t},\ \text{and } u_{i,t}^{G} = \frac{1}{|N_G(i)|}\sum_{j\in N_G(i)} u_{j,t}. \tag{3.2}$$

We combine the Helmert transform in Arellano and Bover (1995) with the between group operation in panel models to transform variables as follows:

$$\begin{aligned} y_{i,t}^{H} &= \sum_{s=t}^{T} h_{s,t}\left(y_{i,s} - y_{i,s}^{G}\right), \\ W_{i,t}^{H} &= \sum_{s=t}^{T} h_{s,t}\left(W_{i,s} - W_{i,s}^{G}\right), \text{ and} \\ u_{i,t}^{H} &= \sum_{s=t}^{T} h_{s,t}\left(u_{i,s} - u_{i,s}^{G}\right), \end{aligned}$$

where $h_{s,t}$'s are constants defined as

$$h_{s,t} = \begin{cases} \sqrt{\dfrac{T-t}{T-t+1}}, & \text{if } s = t \\ -\dfrac{1}{\sqrt{(T-t)(T-t+1)}}, & \text{if } s = t+1, ..., T. \end{cases}$$

Let $Z_{i,t}$ be a d_Z-dimensional vector of instrumental variables, $d_Z \geq d_W$, where d_W denotes the dimension of $W_{i,t}$, and

$$Z^G_{i,t} = \frac{1}{|N_G(i)|} \sum_{i \in N_G(i)} Z_{i,t}.$$

There are multiple ways to choose instrumental variables in our framework. We will discuss this in more detail later. (Conditions for $Z_{i,t}$ are summarized in Assumption 3.1(iv) below.)

We define $n_B = |N_B|$ and $n_F = |N_F|$, so that n_B denotes the number of banks and n_F the number of firms in the sample. For $K \in \{B, F\}$, we construct

$$\hat{A}_{t,K} = \frac{1}{n_K} \sum_{i \in N_K} \sum_{s=t}^{T} h_{s,t}(Z_{i,t} - Z^G_{i,t})(y_{i,s} - y^G_{i,s}),$$

$$\hat{B}_{t,K} = \frac{1}{n_K} \sum_{i \in N_K} \sum_{s=t}^{T} h_{s,t}(Z_{i,t} - Z^G_{i,t})(W_{i,s} - W^G_{i,s})^\top, \text{ and}$$

$$\hat{U}_{t,K} = \frac{1}{n_K} \sum_{i \in N_K} \sum_{s=t}^{T} h_{s,t}(Z_{i,t} - Z^G_{i,t})(u_{i,s} - u^G_{i,s}).$$

By construction, we have

$$\hat{U}_{t,K} = \frac{1}{n_K} \sum_{i \in N_K} \sum_{s=t}^{T} h_{s,t}(Z_{i,t} - Z^G_{i,t})\varepsilon_{i,s}.$$

Hence the Helmert transform eliminates the fixed effects v_i. (The between group transformation eliminates the cluster-specific time effects.)

We let

$$\hat{A}_K = \sum_{t=1}^{T-1} \hat{A}_{t,K}, \text{ and } \quad \hat{B}_K = \sum_{t=1}^{T-1} \hat{B}_{t,K} \tag{3.3}$$

and define our initial estimator of δ_K to be

$$\tilde{\delta}_K = \left(\hat{B}_K^\top \hat{B}_K\right)^{-1} \hat{B}_K^\top \hat{A}_K.$$

Using this, we define $\hat{u}^H_{i,t,K} = Y^H_{i,t} - W^{H\top}_{i,t} \tilde{\delta}_K$, and let

$$\hat{\Omega}_K = \frac{1}{n_K} \sum_{i \in N_K} \left(\sum_{t=1}^{T-1} (Z_{i,t} - Z^G_{i,t}) \hat{u}^H_{i,t,K} \right) \left(\sum_{t=1}^{T-1} (Z_{i,t} - Z^G_{i,t})^\top \hat{u}^H_{i,t,K} \right).$$

Then, we take our estimator of δ_K, $K \in \{B, F\}$, as

$$\hat{\delta}_K = \left(\hat{B}_K^\top \hat{\Omega}_K^{-1} \hat{B}_K\right)^{-1} \hat{B}_K^\top \hat{\Omega}_K^{-1} \hat{A}_K.$$

As we show later, we have

$$\begin{bmatrix} \sqrt{n_B}\hat{V}_B^{-1/2}(\hat{\delta}_B - \delta_B) \\ \\ \sqrt{n_F}\hat{V}_F^{-1/2}(\hat{\delta}_F - \delta_F) \end{bmatrix} \to_d N(0, I),$$

where for $K \in \{B, F\}$,

$$\hat{V}_K = \left(\hat{B}_K^\top \hat{\Omega}_K^{-1} \hat{B}_K\right)^{-1}. \tag{3.4}$$

From the asymptotic normality result, we can obtain the standard error for the k-th parameter of δ_B and δ_F respectively as follows:

$$\hat{\sigma}_{B,k} = \frac{\sqrt{\mathbf{e}_k^\top \hat{V}_B \mathbf{e}_k}}{\sqrt{n_B}}, \text{ and } \hat{\sigma}_{F,k} = \frac{\sqrt{\mathbf{e}_k^\top \hat{V}_F \mathbf{e}_k}}{\sqrt{n_F}},$$

where $\mathbf{e}_k$ denotes the column vector of zeros except for its k-th entry which is one. Thus, for each $K \in \{B, F\}$ and $\alpha \in (0, 1)$, the level $(1-\alpha)$ confidence interval for the k-th parameter of δ_K is given by

$$\left[\hat{\delta}_K - \frac{c_{1-\alpha/2}\hat{\sigma}_{F,k}}{\sqrt{n_K}}, \hat{\delta}_K + \frac{c_{1-\alpha/2}\hat{\sigma}_{F,k}}{\sqrt{n_K}}\right],$$

where $c_{1-\alpha/2}$ denotes the $(1-\alpha/2)$-percentile of the standard normal distribution.

3.2. Instrumental Variables

In this subsection, we discuss various choices of instrumental variables that can be used in practice. The first practical choice is a simple one which takes $Z_{i,t} = W_{i,t}$ for all $t = 1, ..., T$. While this simple choice is legitimate in our context, we may improve the efficiency of the estimator by choosing alternative instrumental variables.

Choice 1: LP (Linear Projection): The following IV is motivated by the optimal IV of Arellano (2003). We consider the following:

$$Z_{i,t} = \left(\sum_{j \in N} W_{j,t}^H \varphi_{j,t}^\top\right)\left(\sum_{j \in N} \varphi_{j,t}\varphi_{j,t}^\top\right)^{-1} \varphi_{i,t},$$

where $\varphi_{j,t} = \varphi_t(W_{j,t} - W_{j,t}^G)$, for some $\mathbf{R}^{d_Z}$-valued function φ_t. The choices of φ_t in practice can be as follows.

(A) $\varphi_t(w_{j,t}) = w_{j,t}$.

(B) $\varphi_t(w_{j,t}) = [w_{j,t}^\top, w_{j,t,1}^2, w_{j,t,2}^2, ..., w_{j,t,d_Z}^2]^\top$.

(C)

$$\varphi_t(w_{j,t}) = \begin{cases} [w_{j,t}^\top, w_{j,t,1}^2, w_{j,t,2}^2, ..., w_{j,t,d_Z}^2]^\top, \text{ if } t = 1 \\ \\ [w_{j,t}^\top, w_{j,t,1}^2, w_{j,t,2}^2, ..., w_{j,t,d}^2, w_{j,t-1,1}^2, w_{j,t-1,2}^2, ..., w_{j,t-1,d_Z}^2]^\top, \text{ if } t > 1. \end{cases}$$

One may include higher order polynomial terms in the definition of IV, but this may induce a severe finite sample bias. In the context of a panel model with cross-sectionally independent observations, the optimal choice of IV has been studied in the literature. (See Donald and Newey (2001) for a general treatment of this problem when there are many choices available for IVs.)

The second choice of IV one may consider is the IV according to the backward orthogonal deviation method proposed by Hayakawa (2009). In a simple form suited to our case, we consider the following choice:

Choice 2: BOD (Backward Orthogonal Deviation): We consider the following IV:

$$Z_{i,t} = \sqrt{\frac{T-t}{T-t+1}} \left(W_{i,t} - \frac{W_{i,t} + ... + W_{i,1}}{t} \right), \ t = 1, ..., T.$$

Hayakawa (2009) showed that in the context of large T asymptotics with cross-sectional independence, this choice yields an estimator whose asymptotic variance is equal to that of an estimator that is based on an infeasible IV.

3.3. Inference on the Direction of Spillover Between Banks and Firms

Let us turn to the problem of detecting the direction of spillovers between banks and firms. Our parameters of focus are now β_{FB} which captures the spillover from firms to banks and β_{BF} which captures the spillover from banks to firms. For simplicity, we assume that $\beta_{FB}, \beta_{BF} \in \mathbf{R}$.

We are interested in testing the following multiple hypotheses:

$$\begin{aligned} H_{0,FB} &: \beta_{FB} = 0, \quad \text{vs} \quad H_{1,FB} : \beta_{FB} \neq 0, \text{ and} \\ H_{0,BF} &: \beta_{BF} = 0, \quad \text{vs} \quad H_{1,BF} : \beta_{BF} \neq 0. \end{aligned}$$

The null hypothesis $H_{0,FB}$ says that there is no spillover from firms to banks and similarly with $H_{0,BF}$. We follow Romano and Wolf (2005) and Romano and Shaikh (2010), and introduce a simple step-down procedure to determine the rejection of the null hypothesis $H_{0,J}$ for each $J \in \{FB, BF\}$, in a way that controls the familywise error rate asymptotically. For this we proceed as follows.

First, we let d be the dimension of $\delta = [\delta_B^\top, \delta_F^\top]^\top$. Define $\hat{\delta} = [\hat{\delta}_B^\top, \hat{\delta}_F^\top]^\top$. Let us introduce two d-dimensional column vectors $\mathbf{e}_{FB}$ and $\mathbf{e}_{BF}$ such that

$$\mathbf{e}_{FB}^\top \delta = \beta_{FB}, \text{ and } \mathbf{e}_{BF}^\top \delta = \beta_{BF}.$$

Hence the vectors $\mathbf{e}_{FB}$ and $\mathbf{e}_{BF}$ select out parameters β_{FB} and β_{BF} from δ. We also define

$$\hat{v}_{FB}^2 = \mathbf{e}_{FB}^\top \hat{V} \mathbf{e}_{FB}, \text{ and } \hat{v}_{BF}^2 = \mathbf{e}_{BF}^\top \hat{V} \mathbf{e}_{BF},$$

where

$$\hat{V} = \begin{bmatrix} \hat{V}_B & 0 \\ 0 & \hat{V}_F \end{bmatrix},$$

and $\hat{V}_K$, $K \in \{B, F\}$, are defined in (3.4). Define

$$\hat{Q}_{FB} = \frac{n_B \hat{\beta}_{FB}^2}{\hat{v}_{FB}^2}, \text{ and } \hat{Q}_{BF} = \frac{n_F \hat{\beta}_{BF}^2}{\hat{v}_{BF}^2}.$$

Note that $\hat{Q}_{FB}$ and $\hat{Q}_{BF}$ are squared t-test statistics from $\hat{\beta}_{FB}$ and $\hat{\beta}_{BF}$.

Now we introduce a procedure to construct a set $\hat{S} \subset \{FB, BF\}$ such that when we reject all the null hypotheses that are outside of this set $\hat{S}$, our decisions are under familywise error rate control asymptotically. For any $\tau \in (0,1)$, we denote c_τ to be the $100\tau\%$ percentile from the distribution of $\chi^2(1)$.

Step 1: Suppose that $\max\left\{\hat{Q}_{FB}, \hat{Q}_{BF}\right\} \leq c_{\sqrt{1-\alpha}}$. Then, we set $\hat{S} = \{FB, BF\}$ and stop.

Step 2: Suppose that $\hat{Q}_{FB} \leq c_{\sqrt{1-\alpha}}$, but $\hat{Q}_{BF} > c_{\sqrt{1-\alpha}}$. Then, we set $\hat{S} = \{FB\}$. On the other hand, suppose that $\hat{Q}_{FB} > c_{\sqrt{1-\alpha}}$, but $\hat{Q}_{BF} \leq c_{\sqrt{1-\alpha}}$. Then, we set $\hat{S} = \{BF\}$.

Step 3: Suppose that $\hat{S} = \{FB\}$ in Step 2. Then, if $\hat{Q}_{FB} > c_{1-\alpha}$, we reset $\hat{S} = \varnothing$ and otherwise we keep $\hat{S} = \{FB\}$. On the other hand, $\hat{S} = \{BF\}$ in Step 2. Then, if $\hat{Q}_{BF} > c_{1-\alpha}$, we reset $\hat{S} = \varnothing$ and otherwise we keep $\hat{S} = \{BF\}$.

Once we obtain the set $\hat{S}$, we perform our hypothesis test as follows. For each $J \in \{FB, BF\}$, we reject the null hypothesis $H_{0,J}$ if and only if $J \notin \hat{S}$.

Following the literature of multiple testing (c.f. Lehmann and Romano (2005), Chapter 9), let us define the familywise error rate (FWER) as follows:

$$\text{FWER}_P = P\left\{H_{0,J} \notin \hat{S}, \text{ for some } J \in \{FB, BF\} \text{ such that } H_{0,J} \in S_P\right\}, \tag{3.5}$$

where $S_P \subset \{FB, BF\}$ is a subset such that $J \in S_P$ if and only if $H_{0,J}$ is true under P. From the asymptotic results below, we can show that

$$\limsup_{n \to \infty} \text{FWER}_P \leq \alpha.$$

Hence this testing procedure controls the familywise error rate asymptotically.

3.4. Asymptotic Theory

In this section, we present the conditions and the results of asymptotic validity of the confidence intervals we have proposed previously. Let us first introduce notation. For each $s = 1, ..., T$, we define

$$\tilde{Z}_{i,s} = \sum_{t=1}^{s\wedge(T-1)} h_{s,t}(Z_{i,t} - Z_{i,t}^G),$$

and for $K \in \{B, F\}$, we let

$$\xi_{s,K} = \frac{1}{\sqrt{n_K}} \sum_{i \in N_K} \tilde{Z}_{i,s}\varepsilon_{i,s}. \tag{3.6}$$

Define $\hat{U}_K = \sum_{t=1}^{T-1} \hat{U}_{t,K}$ and rewrite

$$\sqrt{n_K}(\hat{\delta}_K - \delta_K) = \left(\hat{B}_K^\top \hat{\Omega}_K^{-1} \hat{B}_K\right) \hat{B}_K^\top \hat{\Omega}_K^{-1} \sqrt{n_K}\hat{U}_K.$$

We observe that (see Lemma 1.1 in the appendix)

$$\sqrt{n_K}\hat{U}_K = \sum_{s=1}^{T} \xi_{s,K}, \quad K \in \{FB, BF\}.$$

Hence after removing the fixed effects and cluster-specific time effects through the modified Helmert transform, the random vector $\tilde{Z}_{i,s}$ serves now effectively as our instrumental vector. It is useful to recall that

$$\tilde{Z}_{i,s} = \sqrt{\frac{T-s}{T-s+1}}(Z_{i,s} - Z_{i,s}^G) + \sum_{t=1}^{s\wedge(T-1)} \frac{1}{\sqrt{(T-t)(T-t+1)}}(Z_{i,t} - Z_{i,t}^G).$$

Hence $\tilde{Z}_{i,s}$ does not involve $Z_{j,s}$, for $j \neq i$, and has moments bounded as long as $Z_{i,s}$ has moments bounded uniformly over i.

For the development of the asymptotic theory, let us define $\mathcal{G}_t$ to be the σ-field generated by the neighbors $N_{t,\ell}(i)$, $i \in N$, $\ell = 1, ..., L$. We define

$$\mathcal{F}_t = \sigma\left(W_t, ..., W_0, X_{t+1}, \varepsilon_{t-1}, ..., \varepsilon_0, f_t, f_{t-1}, ..., f_0, \mathcal{G}_{t+1}\right) \vee \mathcal{F}_0,$$

with $f_t = (f_{i,t})_{i\in N}$, $W_t = (W_{i,t})_{i\in N}$, $Z_t = (Z_{i,t})_{i\in N}$, $X_{t+1} = (X_{i,t+1})_{i\in N}$, and $\mathcal{F}_0 = \sigma\left((Y_{i,0}, v_i)_{i\in N}\right)$.

The first set of assumptions is concerned with the error terms $\varepsilon_{i,s}$.

Assumption 3.1. For each $s = 1, ..., T$, the following statement holds.

(i) $\varepsilon_{i,s}$'s are conditionally independent across i given $\mathcal{F}_s$.

(ii) $\mathbf{E}[\varepsilon_{i,s} \mid \mathcal{F}_s] = 0$ for all $i = 1, ..., n$.

(iii) $\max_{i\in N}\mathbf{E}[\varepsilon_{i,s}^4 \mid \mathcal{F}_s] = O_P(1)$ as $n\to\infty$.

(iv) $\sigma^2_{n,\varepsilon,s} = \mathbf{E}[\varepsilon_{i,s}^2 \mid \mathcal{F}_s]$ is identical across $i = 1,...,n$, and as $n\to\infty$, converges in probability to a positive random variable $\sigma^2_{\varepsilon,s} > 0$ which is $\mathcal{F}_0$-measurable.

Assumption 3.1(i) says that once we condition on $\mathcal{F}_s$, $\varepsilon_{i,s}$'s do not exhibit any cross-sectional dependence. Hence the errors can still be cross-sectionally correlated through the variables contained in $\mathcal{F}_s$. Assumption 3.1(iii) requires a conditional fourth moment condition for the errors, uniformly over $i\in N$. Assumption 3.1(iv) allows for conditional heteroskedasticity for $\varepsilon_{i,s}$, only if the heteroskedasticity arises through the conditioning variables in $\mathcal{F}_s$.

The second assumption requires that the instrumental variables are approximated by ones that are constructed from the contemporaneous or past values of $W_{i,t}$'s.

Assumption 3.2. For each $i\in N_K$, $K\in\{B,F\}$ and $t = 1,...,T-1$, there exists a random variable $Z^*_{i,t}$ such that for each $s = t,...,T$,

$$\frac{1}{n_K}\sum_{i\in N_K}\left\|Z_{i,t} - Z^*_{i,t}\right\|^4 = o_P(1), \tag{3.7}$$

and $Z^*_{i,t}$ is an $\mathcal{F}_{t-1}$-measurable function of $(W_{i,t}, W_{i,t-1},....,W_{i,1})$.

This assumption is satisfied immediately if $Z_{i,t} = W_{i,t}$ or if one chooses $Z_{i,t}$ to be one based on backward orthogonal deviation. For the IV's based on the linear projection, we take

$$Z^*_{i,t} = \left(\sum_{j\in N}\mathbf{E}\left[W^H_{j,t}\varphi^\top_{j,t}\mid\mathcal{F}_{t-1}\right]\right)\left(\sum_{j\in N}\mathbf{E}\left[\varphi_{j,t}\varphi^\top_{j,t}\mid\mathcal{F}_{t-1}\right]\right)^{-1}\varphi_{i,t}.$$

Then Assumption 3.2 is satisfied, as long as

$$\begin{aligned}&\left(\sum_{j\in N}W^H_{j,t}\varphi^\top_{j,t}\right)\left(\sum_{j\in N}\varphi_{j,t}\varphi^\top_{j,t}\right)^{-1}\\ &= \left(\sum_{j\in N}\mathbf{E}\left[W^H_{j,t}\varphi^\top_{j,t}\mid\mathcal{F}_{t-1}\right]\right)\left(\sum_{j\in N}\mathbf{E}\left[\varphi_{j,t}\varphi^\top_{j,t}\mid\mathcal{F}_{t-1}\right]\right)^{-1} + o_P(1),\end{aligned}$$

and appropriate moment conditions hold.

The third condition below is a condition requiring the networks to be sparse enough.

Assumption 3.3. There exists $\kappa > 0$ such that for $K\in\{B,F\}$, as $n_K\to\infty$,

$$d_{mx,K} = O_P\left((\log n_K)^\kappa\right),$$

where

$$d_{mx,K} = \max_{i\in N_K}\left|\bigcup_{\ell=1}^L N_\ell(i)\right|, \text{ and } d_{av,K} = \frac{1}{n_K}\sum_{i\in N_K}\left|\bigcup_{\ell=1}^L N_\ell(i)\right|.$$

A similar set of sparsity assumptions have appeared in the literature involving asymptotic normal inference on network models.[10]

The fourth set of assumptions is concerned with the limit of the components in the conditional variance of the estimator $\hat{\delta}$. Using $Z^*_{i,t}$ in Assumption 3.2, we define

$$\tilde{Z}^*_{i,s} = \sum_{t=1}^{s\wedge(T-1)} h_{s,t}(Z^*_{i,t} - Z^{*G}_{i,t}), \text{ with } Z^{*G}_{i,t} = \frac{1}{|N_G(i)|}\sum_{i\in N_G(i)} Z^*_{i,t},$$

and for $K \in \{B, F\}$,

$$\xi^*_{s,K} = \frac{1}{\sqrt{n_K}}\sum_{i\in N_K} \tilde{Z}^*_{i,s}\varepsilon_{i,s}. \tag{3.8}$$

Define

$$B_{n,K} = \sum_{s=1}^{T}\frac{1}{n_K}\sum_{i\in N_K}\mathbf{E}\left[\tilde{Z}^*_{i,s}W^\top_{i,s} \mid \mathcal{F}_{s-1}\right], \text{ and} \tag{3.9}$$

$$\Omega^\circ_{n,s,K} = \frac{1}{n_K}\sum_{i\in N_K}\mathbf{E}\left[\sigma^2_{n,\varepsilon,s}\tilde{Z}^*_{i,s}\tilde{Z}^{*\top}_{i,s} \mid \mathcal{F}_{s-1}\right], \text{ for } s = 1, ..., T,$$

where $\sigma^2_{n,\varepsilon,s} = \mathbf{E}[\varepsilon^2_{i,s} \mid \mathcal{F}_s]$. As for $B_{n,K}$ and $\Omega^\circ_{n,s,K}$, we make the following assumption.

Assumption 3.4. For $K \in \{B, F\}$, as $n_K \to \infty$, for each $s = 1, ..., T$,

$$B_{n,K} \to_P B_K \text{ and } \Omega^\circ_{n,s,K} \to_p \Omega^\circ_{s,K},$$

where both B_K and $\Omega^\circ_{s,K}$ are $\mathcal{F}_0$-measurable, and $B^\top_K B_K$ and $\Omega^\circ_{s,K}$ are all nonsingular.

While this convergence assumption may be replaced by some lower level conditions, it appears that given the heterogeneity of conditional distributions, such convergence seems inevitable for the asymptotic validity of the inference procedure, and has often been used in the literature in developing asymptotic theory with heterogeneously distributed random variables. (For example, see Assumption EX of Kuersteiner and Prucha (2020).)

Lastly, we introduce conditions that control the conditional moments of the data.

Assumption 3.5. There exists $C > 0$ such that for $K \in \{B, F\}$, and for all $n \geq 1$,

$$\sum_{s=1}^{T}\frac{1}{n_K}\sum_{i\in N_K}\mathbf{E}\left[\|\tilde{Z}^*_{i,s}\|^4 \mid \mathcal{F}_{s-1}\right] \leq C, \text{ and } \sum_{s=1}^{T}\frac{1}{n_K}\sum_{i\in N_K}\mathbf{E}\left[\|W_{i,s}\|^4 \mid \mathcal{F}_{s-1}\right] \leq C.$$

Under these assumptions, we can obtain the asymptotic normality for the estimators $\hat{\delta}_B$ and $\hat{\delta}_F$ as follows:

[10] For example, see Assumption 4 of Leung (2020). In fact, Kojevnikov and Song (2021) show that a form of a sparsity condition on a network is necessary for consistent estimation of the long run variance of the sample mean of network dependent observations.

TABLE 1. The Basic Characteristics of Networks Used in the Simulation Study

Bank-Networks.

	BA 1		BA 5		BA 9	
n	500	5000	500	5000	500	5000
maximum degree	63	144	132	452	198	644
average degree	3.91	3.99	19.23	19.92	34.51	35.85

Firm-Networks.

	BA 1		BA 5		BA 9	
n	500	5000	500	5000	500	5000
maximum degree	76	117	149	368	253	626
average degree	3.91	3.99	19.22	19.92	34.52	35.85

Notes: The tables present the network characteristics of the networks used for the simulation study. Bank-Networks refers to the overall characteristics of all units within a bank's in-neighborhood, that is including both firms and other banks. Analogously for the Firm-Networks. The "BA-1", "BA-2", "BA-3"refer to Barabási-Albert graphs, with varied denseness of the graphs.

Theorem 3.1. *Suppose that Assumptions 3.1 -3.5 hold. Then, as* $n_B, n_K \to \infty$,

$$\begin{bmatrix} \sqrt{n_B}\hat{V}_B^{-1/2}(\hat{\delta}_B - \delta_B) \\ \\ \sqrt{n_F}\hat{V}_F^{-1/2}(\hat{\delta}_F - \delta_F) \end{bmatrix} \to_d N(0, I).$$

The asymptotic results show that $\sqrt{n_B}\hat{V}_B^{-1/2}(\hat{\delta}_B - \delta_B)$ and $\sqrt{n_F}\hat{V}_F^{-1/2}(\hat{\delta}_F - \delta_F)$ are asymptotically independent. Our next result shows that the testing procedure based on $\hat{S}$ controls the FWER asymptotically.

Theorem 3.2. *Suppose that Assumptions 3.1-3.5 hold. Let* FWER_p *be as defined in (3.5). Then,*

$$\limsup_{n\to\infty} \mathsf{FWER}_p \leq \alpha.$$

3.5. Monte Carlo Simulations

3.5.1. **Data Generating Process.** We consider a simulation study using the model of spillover between firms and banks described in Section 2.2 above. Let us first explain the data generating process used for this section. In simulations, we choose $n_B = n_F \in \{500, 5000\}$. For the covariates, we simply draw $X_{i,t}$ i.i.d. from $N(\mathbf{1}, I)$ across i's and t's, where $\mathbf{1}$ denotes a vector of ones and $X_{i,t}$ is a p-dimensional random vector with $p = 3$.

As for the error components, we first generate fixed effects, v_i, independently from $N(1, 1)$. For the clusters, we consider equal-size clusters for both banks and firms. In particular, we consider the number of the clusters, G, to be from $\{10, 100\}$ for banks and firms, and the banks have the same number of clusters as the firms. Thus when $G = 100$, the banks have 50

clusters and firms have 50 clusters each. Once cluster structures are determined, we generate cluster-specific time effects $\pi_{t,g}$ which are drawn from $N(1,1)$ independently for each cluster g and time t. Finally we generate idiosyncratic components $\varepsilon_{i,t}$ from $N(0,1)$ independently for each unit i and period t.

For the networks, we use graphs generated based on Barabási-Albert (BA) random graphs with varied denseness, where we generate four BA graphs on the entire cross-sectional units, with each graph representing links from firms to firms, firms to banks, banks to banks and banks to firms. See Table 1 for the network characteristics used in this simulation study. We generate outcomes $y_{i,t}$ according to the model in (2.8). In the generation, we take $T \in \{5,10\}$, and $\gamma_K = 1$ and $\alpha_K, \beta_{KK'} \in \{0,1\}$ for $K, K' \in \{B,F\}$. For the estimation, we simply used the IVs based on the LP with option B. We also report results from using other choices of IVs in the Online Appendix.

3.5.2. **Results.** In order to save space, we present results from the graphs generated using BA random graphs. The results from using ER random graphs are similar. We first focus on the two-sided testing problem of $H_0 : \beta_{FB} = \bar{\beta}_{FB}$ against $H_1 : \beta_{FB} \neq \bar{\beta}_{FB}$ for some values of $\bar{\beta}_{FB}$ we choose. For the test we use a two-sided t-test based on our results of Theorem 3.1. We report the empirical rejection probabilities in Tables 2 and 3, and empirical familywise error rate (FWER) in Table 4, using 5000 Monte Caro simulations.

Table 2 reports the finite sample rejection probabilities under the null hypothesis at levels 0.01, 0.05 and 0.10. First, we note that the finite sample size properties are all reasonably good. As expected, when the sample size increases from $n = 500$ to $n = 5000$, the empirical sizes get closer to the nominal sizes. When T increases from 5 to 10, we have a slight over-rejection with the sample size $n = 500$, but this issue is alleviated when the sample size increases. Most interestingly, the size properties do not exhibit much noticeable difference as the network becomes denser. This suggests that our asymptotic inference performs well with this set of networks.

In Table 3, we present the empirical rejection probabilities under the alternative hypothesis of the following form:

$$H_1 : \beta_{FB} = \bar{\beta}_{FB} + \Delta,$$

for numbers $\Delta > 0$. We choose Δ to be from $\{0.1, 0.5\}$ and use the test at the level 0.05. As expected, when the sample size increases from $n = 500$ to $n = 5000$, the power of the test increases substantially. Also, it is interesting to note that the power increases with the number of the time periods.

However, the power decreases with the denseness of the networks. Such a reduction in power with denser networks has been observed in the literature. (See Kojevnikov, Marmer,

TABLE 2. Empirical Rejection Probabilities under the Null Hypothesis

$\bar{\beta}_{FB} = 0$, $\alpha_B = \alpha_F = 0$, and $\beta_{BF} = \beta_{BB} = \beta_{FF} = 0$

		BA 1		BA 5		BA 9	
n	α	$T=5$	$T=10$	$T=5$	$T=10$	$T=5$	$T=10$
500	0.01	0.016	0.014	0.014	0.016	0.019	0.014
	0.05	0.055	0.064	0.066	0.062	0.074	0.067
	0.10	0.114	0.122	0.120	0.113	0.129	0.120
5000	0.01	0.009	0.011	0.01	0.011	0.010	0.010
	0.05	0.047	0.053	0.053	0.045	0.048	0.05
	0.10	0.098	0.101	0.108	0.096	0.102	0.099

$\bar{\beta}_{FB} = 1$, $\alpha_B = \alpha_F = 1$, and $\beta_{BF} = \beta_{BB} = \beta_{FF} = 1$

		BA 1		BA 5		BA 9	
n	α	$T=5$	$T=10$	$T=5$	$T=10$	$T=5$	$T=10$
500	0.01	0.012	0.015	0.014	0.015	0.015	0.016
	0.05	0.059	0.068	0.062	0.063	0.069	0.065
	0.10	0.114	0.121	0.117	0.118	0.124	0.124
5000	0.01	0.01	0.009	0.010	0.011	0.010	0.010
	0.05	0.05	0.048	0.049	0.055	0.050	0.050
	0.10	0.100	0.104	0.107	0.107	0.099	0.104

$\bar{\beta}_{FB} = 1$, $\bar{\beta}_{BF} = 0$, with $\alpha_B = \alpha_F = 1$, and $\beta_{BB} = \beta_{FF} = 0$

		BA 1		BA 5		BA 9	
n	α	$T=5$	$T=10$	$T=5$	$T=10$	$T=5$	$T=10$
500	0.01	0.011	0.016	0.015	0.014	0.016	0.016
	0.05	0.065	0.069	0.070	0.071	0.069	0.074
	0.10	0.119	0.125	0.133	0.131	0.134	0.131
5000	0.01	0.009	0.01	0.012	0.011	0.01	0.012
	0.05	0.056	0.050	0.056	0.047	0.054	0.054
	0.10	0.106	0.098	0.107	0.102	0.106	0.104

Notes: The table presents the empirical rejection probability under the null hypothesis that $\beta_{FB} = \bar{\beta}_{FB}$, where we choose $\bar{\beta}_{FB} = 0$ or $\bar{\beta}_{FB} = 1$. As before, the "BA-1", "BA-2" and "BA-3" represent the graphs generated according to Barabási-Albert graphs with varied denseness. The numbers $\alpha = 0.01, 0.05, 0.10$ denote the nominal level of the test used in this study. The Monte Carlo simulation number was 5,000.

and Song (2021).) In many situations, the reduction in power happens due to an increase in the cross-sectional dependence of the observations. This increase is captured during the HAC (Heteroskedasticity-Autocorrelation Consistent) estimation of the asymptotic variance, and this estimator usually depends on the network. However, in our case, our asymptotic variance estimator does not involve networks. Furthermore, even when all the parameters are set to be zero, that is, there is no cross-sectional dependence created along the network, the power of the test decreases with the denseness of the network. This suggests that the reduction in power in this case is not due to the increase in the cross-sectional dependence

TABLE 3. Empirical Rejection Probabilities under the Alternative Hypothesis: $\beta_{FB} = \bar{\beta}_{FB} + \Delta$ at the Nominal Level 0.05

$\bar{\beta}_{FB} = 0$, $\alpha_B = \alpha_F = 0$, and $\beta_{BF} = \beta_{BB} = \beta_{FF} = 0$

		BA 1		BA 5		BA 9	
n	Δ	$T=5$	$T=10$	$T=5$	$T=10$	$T=5$	$T=10$
500	0.10	0.999	1.000	0.638	0.956	0.433	0.788
	0.5	1.000	1.000	1.000	1.000	1.000	1.000
5000	0.10	1.000	1.000	1.000	1.000	1.000	1.000
	0.5	1.000	1.000	1.000	1.000	1.000	1.000

$\bar{\beta}_{FB} = 1$, $\alpha_B = \alpha_F = 1$, and $\beta_{BF} = \beta_{BB} = \beta_{FF} = 1$

		BA 1		BA 5		BA 9	
n	Δ	$T=5$	$T=10$	$T=5$	$T=10$	$T=5$	$T=10$
500	0.10	1.000	1.000	0.276	1.000	0.111	0.993
	0.5	1.000	1.000	1.000	1.000	0.973	1.000
5000	0.10	1.000	1.000	0.991	1.000	0.709	1.000
	0.5	1.000	1.000	1.000	1.000	1.000	1.000

$\bar{\beta}_{FB} = 1$, $\bar{\beta}_{BF} = 0$, with $\alpha_B = \alpha_F = 1$, and $\beta_{BB} = \beta_{FF} = 0$

		BA 1		BA 5		BA 9	
n	Δ	$T=5$	$T=10$	$T=5$	$T=10$	$T=5$	$T=10$
500	0.10	0.310	0.897	0.081	0.330	0.071	0.261
	0.5	1.000	1.000	0.897	1.000	0.822	1.000
5000	0.10	0.666	1.000	0.38	0.99	0.331	0.977
	0.5	1.000	1.000	1.000	1.000	1.000	1.000

Notes: The table shows the empirical rejection probability under the alternative hypothesis that $\beta_{FB} = \bar{\beta}_{FB} + \Delta$ at the nominal level 0.05, where we choose $\bar{\beta}_{FB} = 0$ or $\bar{\beta}_{FB} = 1$, and $\Delta \in \{0.1, 0.5\}$. As before, the "BA-1", "BA-2" and "BA-3" represent the graphs generated according to Erdös-Rényi graphs with different configurations of the denseness of the networks. The Monte Carlo simulation number was 5,000. As expected, the power of the test increases with the sample size. It is also worth noting that it also increases substantially as the time T increases from $T = 5$ to $T = 10$. Most importantly, as the network becomes denser, the power decreases.

of the observations. In fact, this is due to the decrease in the variations of $\overline{y}_{i,t}$ as the network becomes denser. Recall that $\overline{y}_{i,t}$ is the average of the outcomes of the neighbors of unit i. When the size of the neighborhood increases, and the outcomes are weakly dependent and distributionally similar, as in our simulation design, the law of large numbers can reduce the variations of $\overline{y}_{i,t}$, as the network becomes denser, eventually, leading to the weak power. We expect that this reduction in power will be alleviated when the heterogeneity in distribution of the outcomes is large.

Finally, we investigate the finite sample performance of the multiple testing procedure explained in Section 3.3. In particular we consider two settings. The first setting focuses on the case with $\beta_{FB} = 0.0$ and $\beta_{BF} = 0.5$, so that we have $S_P = \{FB\}$, and the second setting

TABLE 4. Empirical Familywise Error Rate

$\bar{\beta}_{FB} = 0$, $\bar{\beta}_{BF} = 0$, with $\alpha_B = \alpha_F = 0$, and $\beta_{BB} = \beta_{FF} = 0$

		BA 1		BA 5		BA 9	
n	α	$T=5$	$T=10$	$T=5$	$T=10$	$T=5$	$T=10$
500	0.01	0.018	0.017	0.017	0.018	0.017	0.017
	0.05	0.065	0.072	0.069	0.070	0.071	0.069
	0.10	0.118	0.130	0.129	0.127	0.133	0.130
5000	0.01	0.009	0.011	0.011	0.011	0.009	0.010
	0.05	0.047	0.055	0.052	0.052	0.047	0.052
	0.10	0.094	0.108	0.101	0.093	0.093	0.105

$\bar{\beta}_{FB} = 1$, $\bar{\beta}_{BF} = 0$, with $\alpha_B = \alpha_F = 1$, and $\beta_{BB} = \beta_{FF} = 0$

		BA 1		BA 5		BA 9	
n	α	$T=5$	$T=10$	$T=5$	$T=10$	$T=5$	$T=10$
500	0.01	0.013	0.012	0.015	0.017	0.011	0.015
	0.05	0.057	0.060	0.062	0.060	0.059	0.066
	0.10	0.115	0.125	0.122	0.122	0.113	0.124
5000	0.01	0.012	0.009	0.012	0.011	0.010	0.010
	0.05	0.053	0.050	0.055	0.054	0.050	0.050
	0.10	0.103	0.101	0.111	0.099	0.102	0.098

Notes: The table presents the empirical familywise error rate (FWER) for the step down procedure explain in Section 3.3. The nominal FWER is given by $\alpha = 0.01, 0.05, 0.10$.

focuses on the case with $\beta_{FB} = 0$ and $\beta_{BF} = 0.0$, so that we have $S_P = \{FB, BF\}$. In Table 4, we report the finite sample FWER of the multiple testing procedure, as the empirical average of the incidence of $\hat{S}$ failing to contain S_P as a subset. The results show that the finite sample performance of the FWER is reasonable. When the sample sizes are large, the finite sample FWER gets closer to its nominal counterparts.

Let us summarize our findings from the Monte Carlo simulation study. First, the finite size properties of the tests are quite stable, regardless of the denseness of the networks used in this study. However, when the network becomes denser, the power of the tests gets weaker, and this is mostly due to the reduced variation of the prior average outcomes over the neighborhood. Second, the power of the tests increases with the sample size n and the number of the time periods T. Third, the finite sample FWER performs reasonably well across the network configurations and time periods.

4. Empirical Analysis of Spillover between Industrial Sector Outcomes and Bank Weakness

4.1. Data

In order to put our methodology to the test, we collect detailed data from Spain between 2005 and 2012 which links narrow sectors of real economic activity to the credit institutions providing them with external funding.

Our sector-level data is derived from annual firm-level balance sheets from Bureau van Dijk's (BvD) Orbis dataset. The coverage of the firm-level data is comprehensive: firms in the sample account for 69-82% of Spanish gross output in the period 2005-2012 and the share of activity accounted for by small, medium and large firms closely resembles that observed in aggregate data.[11] We drop firm-year observations with non-positive values for total assets, tangible fixed assets, and number of employees as well as entries with negative liabilities and net worth. We drop firms in the financial sector (NACE Rev. 2 codes 64-66) and only keep observations for which basic accounting identities are satisfied.[12] Nominal quantities are deflated using sector-specific GDP deflators from Eurostat.

In order to match firms to their banks, we exploit the banker variable in Orbis, which reports the names of up to ten credit institutions with which the firm has a relationship. We take the fact that a firm reports the name of a bank to also mean that the bank lends to the firm, an assumption commonly made in the literature on firm-bank relationships.[13] The banker variable does not include a time stamp, meaning that we cannot determine when a lending relationship started or whether it changed over time. This shortcoming is mitigated by evidence that lender-borrower relationships tend to be sticky over the business cycle.[14]

We match the bank names reported in the firm-level data with bank financial statements from BvD's Bankscope dataset.[15] We exclude credit institutions specializing in consumer credit, such as credit card and leasing companies, as well as private security and asset management companies. We construct our yearly panel of banks so as to maximize both the number of banks and the number of time periods, as both dimensions are important for our methodology. To do so, we prioritize unconsolidated accounts over consolidated ones where

[11] See Kalemli-Ozcan, Sorensen, Villegas-Sanchez, Volosovych, and Yesiltas (2015). 2006 gross output shares for small (<19 employees), medium ($20-249$ employees) and large (>250 employees) firms are, respectively, $(0.22, 0.39, 0.40)$ in the Orbis data and $(0.21, 0.38, 0.41)$ if the aggregate data from Eurostat.

[12] The criteria are as in Gopinath, Kalemli-Ozcan, Karabarbounis, and Villegas-Sanchez (2017).

[13] See, for example, Kalemli-Ozcan, Laeven, and Moreno (2022) and Laeven, McAdam, and Popov (2018) who also infer a lending relationship from the same data source.

[14] Giannetti and Ongena (2012) look at different vintages of the banker variable and find it to be very persistent. Chodorow-Reich (2014) finds consistent evidence using different data from the U.S.

[15] The matching is done based on names for lack of a common identifier in the two data sources.

possible, while making sure to avoid double-counting issues.[16] By using unconsolidated accounts we also avoid the possibility that variation at the individual bank level is lost at the consolidated level.

After cleaning the data according to the procedure outlined above, we are left with 188, 923 unique firms matched to 97 unique banks and operating in 600 three-digit NACE Rev 2. sectors. The number of cross-sectional units underlying the main results in Section 4.5 are lower because our estimation procedure requires strongly balanced panels. To mitigate the loss of observations, we interpolate gaps in our variables of interest of up to three years.

The following section details the definitions of the variables of interest for our spillover analysis and presents some basic stylized facts.

4.2. Definitions and Stylized Facts

Zombie lending is the practice of extending credit to distressed firms that would exit the market under normal conditions. The incentive to evergreen loans to ailing firms is especially strong for weak banks seeking to avoid further damaging their balance sheet by reporting their losses.

Zombie Firms. Several ways of identifying zombie firms have been proposed in the literature, and they are all designed to capture persistent financial weakness of the firm and/or the extent to which the firm is receiving subsidized credit. In this paper we follow Adalet McGowan, Andrews, and Millot (2018) and use a definition based on the interest coverage ratio defined as the ratio of profits (EBIT) to interest payments. According to this definition, a firm is considered a zombie in a given year if it has reported an interest coverage ratio below one for three consecutive years. This definition, which we will refer to as the baseline definition, states that a zombie firm is not profitable enough to make its debt payments. We interpret the fact that such firms are kept afloat as evidence of bank forbearance.

It is worth pointing out that our baseline measure, unlike the one proposed by Caballero, Hoshi, and Kashyap (2008) or Acharya, Eisert, Eufinger, and Hirsch (2019), does not seek to identify firms receiving subsidized credit, that is, firms paying lower interest rates than their most creditworthy counterparts. The reasons behind this are twofold. First, we do not have information on the interest rates on individual loans, so we would have to infer the "average" interest rate paid by a firm from the ratio of interest payments to total debt. Second, we would need an appropriate benchmark to compare our interest rate proxy to. Other papers use the interest rate paid by AAA-rated publicly listed firms for this purpose, however, this benchmark

[16] We follow the steps outlined in Duprey and Le (2016) to create consistent time series.

TABLE 5. Firm characteristics by zombie status

	Non-zombie		Zombie	
	Mean	Median	Mean	Median
Firm age	15.172	14.000	17.293	16.000
Total assets (million euro)	3.040	0.757	4.782	1.003
Sales (million euro)	2.700	0.697	1.987	0.362
Number of employees	16.707	7.000	16.238	5.000
Return on assets	0.020	0.014	−0.060	−0.031
Investment ratio	0.429	−0.045	0.224	−0.039
Leverage ratio	0.270	0.223	0.315	0.273
Interest coverage ratio	210.656	2.119	−385.585	−2.764
Debt service capacity	39.113	0.324	−15.119	−0.001
Exit	0.089	0.000	0.113	0.000
Observations	1,309,561		135,573	

Notes: This table shows a break-down of firm characteristics by zombie status according to the baseline definition. The sample period is 2005-2012. The return on assets is the ratio of net income to total assets; the investment ratio is the percent change in real fixed assets from the year before; the leverage ratio is the ratio of total debt to total assets; the interest coverage ratio is the ratio of profits to the amount of interest paid; the debt service capacity is the ratio of profits to total debt; exit is an indicator equal to one if a firm is dissolved or declares bankruptcy in the future.

is hardly relevant for our sample which mainly consists of unlisted, small- to medium-sized enterprises which are very different from large public corporations.[17]

Table 5 summarizes some firm characteristics by zombie status. We can see that zombie firms, on average, exhibit markedly lower sales, profitability, and investment while at the same time being more leveraged and more likely to exit. Zombie firms are also older.[18]

Weak Banks. Our choice of a variable to capture bank weakness is informed by the previous literature on zombie lending and on the bank lending channel more generally. Some papers, such as Acharya, Eisert, Eufinger, and Hirsch (2019), define weak banks to be those with a low ratio of regulatory capital, while others build on that to create an index which includes additional balance sheet items such as non-performing loans (Storz, Koetter, Setzer, and Westphal (2017), Andrews and Petroulakis (2019)). A different approach relies on the receipt of government aid (Laeven, McAdam, and Popov (2018), Acharya, Borchert, Jager, and Steffen (2021)), while yet another is to exploit the decline in the creditworthiness of some European sovereigns during 2010-2012 to measure bank weakness as the exposure to risky government debt (Kalemli-Ozcan, Laeven, and Moreno (2022)).

[17]To get a sense of how exceptional listed firms are in Spain, the average value-added share of listed firms in manufacturing was approximately 14% in 2006 (Garcia-Macia (2017)).

[18]Some zombie firm definitions also impose a firm age of over ten years to avoid misidentifying potentially successful start-ups as zombies. However, less than 25% of observations attributed to zombies come from firms under ten years of age so we omit this criterion.

TABLE 6. Bank outcome: Correlation with other characteristics

	Loan loss provisions		
	Corr.	p-value	Obs.
Return on avg. assets	−0.104	0.000	1246
Return on avg. equity	−0.065	0.021	1244
Capital ratio (equity to assets)	0.179	0.000	1246
Loan loss reserves (share of gross loans)	0.316	0.000	513
Sovereign exposure (share of total assets)	0.114	0.023	396
Non-performing loans (share of gross loans)	0.136	0.008	378

Notes: This table shows the correlation between our baseline measure of bank weakness, given by the share of loan loss provisions in gross loans, and other bank characertistics. The sample period is 2005-2012.

The ideal measure of bank weakness in the context of our methodology is one that, in addition to capturing balance sheet vulnerability, also displays substantial within-bank time variation and is available for many banks, especially for smaller ones. We therefore settle for the ratio of loan loss provisions to gross loans as our preferred bank weakness measure. Loan loss provisions are an expense set aside by banks to cover different kinds of loan losses, including non-performing loans. The loan loss provisions are then added to the loan loss reserves, which banks are required to maintain as a buffer against potential future losses.

Table 6 shows how our bank weakness measure is related to other bank characteristics. Bank weakness is negatively correlated with profitability, as proxied by the return on average assets and the return on average equity. Weaker banks also have larger sovereign bond holdings, which is not surprising given that our sample period contains the European sovereign debt crisis.[19] Somewhat surprisingly, banks reporting higher loan loss provisions also seem to be better capitalized. While a higher capital ratio is generally considered a sign of a healthy balance sheet, Andrews and Petroulakis (2019) point out that it could also be the result of low risk-taking and little lending activity. Conversely, banks possessing high-quality assets which generate a steady flow of income with limited risk may afford to have relatively lower levels of capital adequacy.[20]

It should be noted that, ultimately, any balance sheet item is subject to manipulation on the part of the bank, as documented by Blattner, Farinha, and Rebelo (2019) using granular loan-level data from Portugal. This is why, in a future extension of the paper, we will explore measuring bank weakness through government aid. More work needs to be done to make such a variable continuous and time-varying.

[19]The sovereign debt variable in Bankscope includes the debt of all sovereigns, not just that of the home country. However, in the case of Spain, most of the sovereign debt held by banks was that of the Spanish government.

[20]A better capital-based measure would be one based on risk-weighted capital or Tier 1 capital ratios, however, both these variables are riddled with data availability issues in our sample.

FIGURE 1. Evolution of outcomes over time

(A) Bank outcome

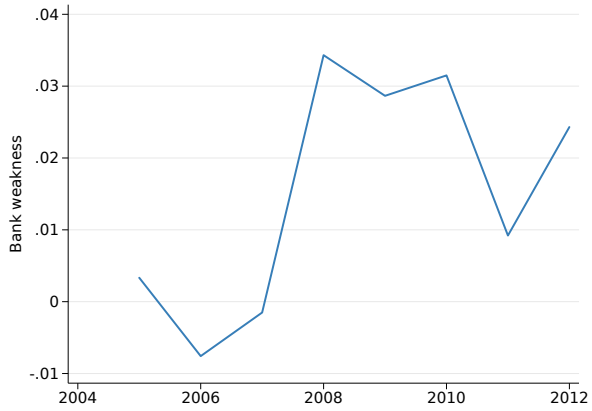

(B) Sector outcome

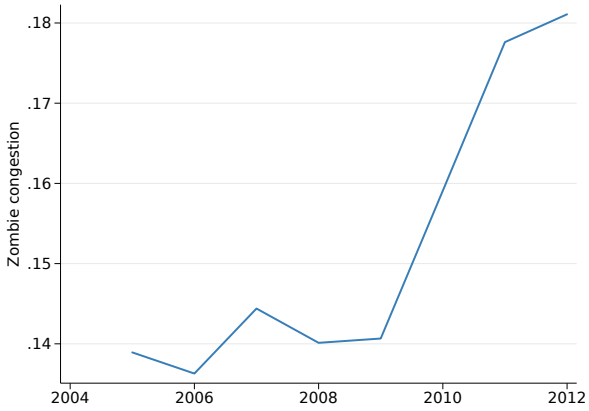

Notes: This figure plots the outcomes of interest over time. Panel (a) plots bank weakness as measured by the average loan loss provision ratio, while Panel (b) plots sector-level zombie congestion as measured by the asset-weighted share of zombie firms in each sector according to the baseline definition.

Figure 1 plots the time averages of the our main outcome variables: Panel (a) refers to the bank outcome measured by the loan loss provision share, while Panel (b) shows the asset-weighted average of zombie firms based on the interest-coverage definition. We can see that both measures vary significantly over our sample period and that a surge in bank weakness around 2008 is followed by an increase in sectoral zombie-firm congestion two years later.

4.3. Networks

Having fixed our outcomes of interest at both the bank and the sector level, we now move on to defining the network structure governing the spillover between these outcomes.

Identifying the networks along which we expect sector-level outcomes to have an effect on bank performance and vice versa is a crucial part of our analysis. This section is devoted to a careful discussion of how to define the networks which best capture the causal channels going from sectors to banks and from banks to sectors.

At its core, the interdependence between the real sector and the financial sector comes from the former borrowing from the latter. It makes sense, then, to assume that a firm is related to a bank if the firm borrows from that bank. However, when we move past the level of the individual firm and look at the sector in which the firm is active, the exact definition of what it means for that sector to be tied to the bank becomes less clear-cut. In what follows, we take each spillover direction in turn and discuss the associated network definition.

Sector to Bank For the sector-to-bank spillover, we want to explain a bank's health using the share of distressed firms in the sectors that the bank caters to. Some sectors will be more

FIGURE 2. Network characteristics (25th prc.)

(A) Sector to bank

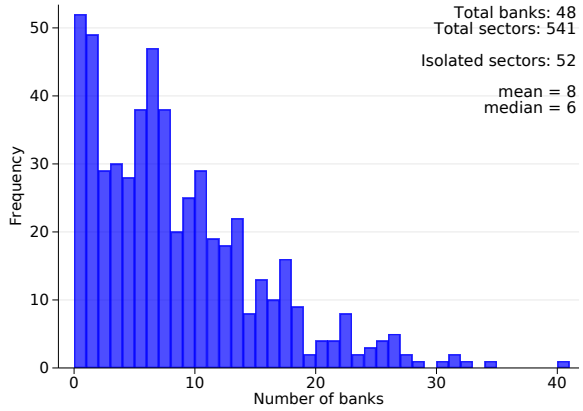

(B) Bank to sector

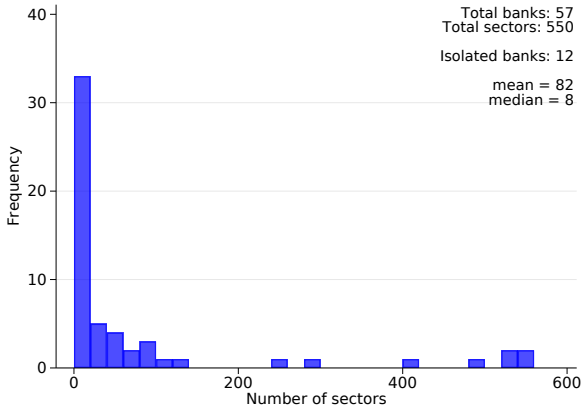

Notes: This figure shows the network characteristics for the baseline specification. Panel (a) shows the distribution of the number of sectors per bank, while Panel (b) shows the distribution of the number of banks per sector. The network thresholds in Panels (a) and (b) are set to the 25th percentile of the relevant debt share and asset share, respectively.

important for a bank than others, so we should only expect spillover to occur if a bank is sufficiently exposed to a given sector. A natural measure of exposure to a given sector can be obtained by looking at what share in the total amount of loans originating from a bank goes to that sector. A bank's solvency relies on the ability of its borrowers to pay back their debt, so if a bank is heavily invested in a sector where many firms are experiencing financial distress, then we should expect that bank to suffer losses.

This definition of exposure makes sense in light of the bank and sector outcomes we are interested in. On the bank side, we are interested in bank health as measured by the provisions set aside by the bank to absorb losses from missed loan payments. On the sector side, we are interested in the prevalence of zombie firms as measured by a chronic inability to make interest payments on their debt.

Ideally, we would derive our exposure measure from loan-level data which would contain the identity of the bank, the identity of the firm and the firm's sector of activity. Unfortunately, our data does not possess this level of granularity since we do not observe a bank's individual loans or their breakdown by sector. We do, however, observe firms' total amount of debt and sector of activity as well as the identity of the banks they are related to.[21]

We define a sector-to-bank relationship based on the share of a sector's debt in the total debt associated with a bank, measured in the year before our sample starts. If that share is

[21]Around 36% of firms in our sample report more than one bank. We use all bank relationships for our baseline specification, but we will also explore the robustness of our results to using only the first bank mentioned by each firm.

higher than the 25th percentile of all bank-sector pairs, we assume that the sector potentially affects the bank.

Bank to Sector For the bank-to-sector spillover, we want to explain the degree of a sector's zombie congestion using the health of its main lenders. Following a similar logic as above, we would expect a bank to matter for a sector if the bank lends to a sizable segment of that sector. Given that we are interested in measuring a bank's impact on a sector, and that our sector-level outcome is the asset-weighted share of zombie firms, it makes sense to look at the asset share in that sector that is accounted for by that bank.

We define a bank-to-sector relationship based on the share of a sector's assets belonging to the firms which borrow from a bank, measured in the year before our sample starts. If that share is higher than the 25th percentile of all bank-sector pairs, we assume that the bank potentially affects the sector.

The choice of threshold for both spillover directions is faced with the following trade-off: the higher the threshold, the more sparse our network structure will be and the more statistical power our estimation will have; however, a higher threshold also means dropping smaller banks or sectors from the analysis, which could introduce a bias. Figure 2 summarizes the network characteristics for both directions for a threshold set to equal the 25th percentile of the relevant debt share (in the sector-to-bank direction) and asset share (in the bank-to-sector direction), which our empirical analysis has chosen to focus on. In the Online Appendix, we report results from different choices of the threshold.

4.4. Specification Details

We are now equipped with a sector- and a bank-level outcome, as well as with a set of directed networks along which to analyze the spillover between the two outcomes. It remains to discuss the control variables for our regressions.

Both regressions of the bank-to-sector and the sector-to-bank equations include the lagged outcome as well as time- and individual-specific fixed effects. Here we assume that the cluster structure on the cross-sectional units coincides with their partition into banks and sectors. Hence cluster-specific time effects consist of two kinds of time effects, one that is common among banks and the other that is common among sectors. These time effects absorb any variation that is common across all banks or all sectors in a given year, such as adverse aggregate demand shocks. Similarly, individual sector (bank) effects control for any time-invariant characteristics that may influence sector (bank) performance. In the case of sectors, such characteristics could include the extent of government regulation, while for banks they could be management practices or overall institutional quality.

TABLE 7. Summary statistics

	Mean	Std. dev.	5th prc.	50th prc.	95th prc.
Bank weakness	0.008	0.040	0.001	0.005	0.026
Zombie congestion	0.142	0.125	0.019	0.103	0.404
Market concentration	0.040	0.088	0.001	0.013	0.153
Sales growth	−0.020	0.175	−0.282	0.005	0.162
Capital intensity	0.729	1.230	0.133	0.356	2.555
Observations	35,144				

Notes: This table shows summary statistics of the variables included in the baseline estimation. The sample consists of bank-to-sector pairs observed between 2005 and 2012. Bank weakness is given by the ratio of loan loss provsions to total assets; zombie congestion is the asset-weighted share of zombie firms in a sector according to the baseline definition; market concentration is the HHI index of sector-level sales; sales growth is computed as the log difference in total sector sales from the year before; capital intensity is the share of a sector's fixed assets in total sales.

In the bank-level equation, we opt for the most parsimonious specification which only includes the lagged outcome and the time- and bank effects. The reason behind this is that most bank assets and liabilities are not marked to market, meaning that these balance sheet variables are very stable and do not register large enough movements over time to distinguish them from the time-invariant effects. Including additional controls would also reduce our sample size while providing little in terms of explanatory power.

In the sector-level equation, the richness of our data permits the inclusion of additional time-varying controls. We control for previous-period market concentration (Herfindahl index), sales growth, and capital intensity (share of fixed assets). A priori, a higher market concentration could affect the zombie share in a sector either positively – by distorting competition – or negatively – by favoring large firms with high enough profit margins that make them more resilient to shocks. As for sales growth, we would expect it to have a negative impact on zombie congestion, since a boost in sales can provide firms with a buffer that insulates them against falling behind on loan payments. Finally, capital intensity is meant to capture the degree to which a sector is dependent on banks. We include this control to make sure that it is the characteristics of the banks driving the zombie share, and not the sector's intrinsic reliance on banks. Table 7 provides summary statistics of our outcome and control variables.

4.5. Results

Our main results are shown in Table 8. Panel A refers to the bank-level equation where we are interested in how the sector-level zombie share affects bank weakness. Panel B refers to the sector-level equation where we are interested in the opposite spillover direction. In

TABLE 8. Baseline specification (using IV based on LP with option B)

	Coef.	Std. err.	p-value	[95% Conf.	interval]
Panel A: Sector to bank					
Bank weakness $_{t-1}$	0.330	0.002	0.000	0.326	0.334
Zombie congestion $_{t-1}$	0.964	0.322	0.003	0.333	1.596
Number of banks	48				
Number of sectors	541				
Observations	35 144				
Panel B: Bank to sector					
Zombie congestion $_{t-1}$	0.698	0.049	0.000	0.603	0.793
Bank weakness $_{t-1}$	0.138	0.047	0.003	0.046	0.230
Market concentration $_{t-1}$	−0.025	0.099	0.803	−0.218	0.169
Sales growth $_{t-1}$	−0.001	0.008	0.908	−0.016	0.014
Capital intensity $_{t-1}$	−0.015	0.009	0.092	−0.031	0.002
Number of banks	57				
Number of sectors	550				
Observations	37 448				
Direction of spillover with FWER control	$S \longleftrightarrow B$	at 1%			

Notes: This table shows the results from estimating equation (2.8). Panel A refers to the direction from sectors to banks while Panel B refers to the direction from banks to sectors. The network thresholds in Panels A and B are set to the 25th percentile of the relevant debt share and asset share, respectively. The sample contains all reported firm-bank relationships and covers the period between 2005 and 2012. Results are obtained using using IVs based on Linear Projection with Option B. Bank weakness is given by the ratio of loan loss provsions to total assets; zombie congestion is the asset-weighted share of zombie firms in a sector according to the baseline definition; market concentration is the HHI index of sector-level sales; sales growth is computed as the log difference in total sector sales from the year before; capital intensity is the share of a sector's fixed assets in total sales.

both panels, the first row represents the persistence of the outcome and the second row is our main coefficient of interest.

Focusing first on the sector-to-bank direction (Panel A), we see that a higher level of zombie congestion in a bank's neighboring sectors leads to a significant increase in bank weakness. To get a sense of the magnitude of the effect, note that the average zombie share increased by about 4 percentage points from peak to trough (see Figure 1). Such an increase in the zombie share translates to a an increase in the bank's loan loss provisions of $4 \times .96 = 3.8$ percent of gross loans. This means that banks tied to sectors where resources are tied up in distressed firms suffer bigger losses.

Turning now to Panel B, we see that the spillover effect is still highly significant when looking at the bank-to-sector direction. Weaker banks lead to a significant increase in the prevalence of zombie firms in their neighboring sectors. An increase of 4 percentage points in the loan loss provision share of a bank (as was observed on average from peak to trough)

leads to a $4 \times .14 = .6$ percentage point increase in a sector's share of resources sunk in zombie firms. Interestingly, the control variables do not appear to play a significant role explaining the next period zombie share of the sectors.

Our evidence suggests that there is significant spillover originating from banks to sectors, as well as from sectors to banks.

4.6. Robustness

Here we explore how our results vary as we modify specifications of networks and instruments. To save space, we provide a summary of the results here, and present details of the results in the Online Appendix.

4.6.1. **Varying Networks.** As a robustness check, we first varied the denseness of the networks, by taking a threshold of 10 percent to generate a denser network, and a threshold of 50 percent for a sparser network. (See Figures 3 and 4 for the summary of network statistics and Tables 19 and 18 for results in the Online Appendix). When we used the denser network, the results remain robust; both directions of the spillover between banks and sectors are positive with statistical significance at 1%. Interestingly, when we used the sparser network, the spillover from banks to sectors becomes statistically insignificant whereas the spillover from sectors to banks remain significant. This change mostly stems from the links eliminated from the network rather than from a reduction of the set of banks and sectors, which suggests that by using the sparser network, one loses information on the spillover from banks to sectors.

Second, we considered an alternative definition of links from banks to sectors, which is based on debt, rather than assets. More specifically, bank i is linked to sector j if the firms in sector j with which bank i has a relationship account for more than the 25% percentile of the shares for all firms in sector j. We believe that this alternative definition is less reasonable than our previous choice; for example, if there is a large zombie firm (in terms of assets) in sector j and that firm is tied to a weak bank, but at the same time, the debt of that firm is not too high, then it would appear that the zombie congestion in sector j (which will be very large because the firm is very large) is unrelated to the bank's weakness when in fact it is. Nevertheless, we followed our estimation procedure using this specification for a robustness check. The result is reported in Table 20 in the Online Appendix. While the spillover from banks to sectors remains positive, the statistical significance is reduced from a p-value of 0.003 to 0.146. This appears to suggest that the spillover from banks to sectors is better captured using asset-based links rather than debt-based links.

4.6.2. **Varying Instruments.** In the baseline specification, we considered the IVs based on Linear Projection with Option B. We also obtained estimates using Options A and B. Recall

that Option A uses just-identification, taking $Z_{i,t} = W_{i,t}$ and Option C uses overidentification like the baseline specification but with more IVs based on the past values of $W_{i,t}$. The results are reported in Tables 22 (with Option A) and 23 (with Option C).

When we use Option A, the result shows that while the spillover from banks to sectors remains almost the same, the positive spillover from sectors to banks exhibits reduced statistical significance from a p-value of 0.003 to 0.133. This suggests that the quadratic transformation of $W_{i,t}$ as IVs is strongly relevant for explaining the spillover from sectors to banks. On the other hand, when we used Option C, the statistical significance of positive spillovers between the banks and the sectors is restored at 5% in both directions.

4.6.3. **Alternative Definition of Bank Relationships.** As mentioned previously, we have estimated the same model but using the sector-bank networks resulting from only using the first reported bank relationship for each firm. Other papers in the literature restrict their attention to the first bank named by each firm based on the assumption that the ranking of the firm's banks represents the strength of the relationship (see Ferrando, Popov, and Udell (2019) for example). The results are shown in Table 21. The spillover effect from banks to sectors remains significant at the 1% level. In the opposite direction, however, the coefficient is still positive but no longer significant. This could be due to the resulting smaller number of linked sector-bank pairs which leads to a loss of statistical power.

5. Conclusion

In many empirical settings, a researcher is interested in the influence of the outcomes of one group of units on those of another group. However, in many such settings, it is also plausible that the influence in the other direction also exists. In such a situation, we would like to have an empirical model where the directions are assigned a separate role in the model. In this paper, we introduce a new approach of empirical modeling through the use of multiple networks in the context of dynamic linear panel models, and develop asymptotic inference on those spillover effects. Our method is quite simple to use, and shown to perform very well in finite samples in Monte Carlo simulations.

Using bank-firm data from Spain, we demonstrate how our methodology can be harnessed to measure the spillover effects between banks and sectors, with the direction of spillover explicitly distinguished in the model. From the analysis, we find that there is positive spillover between banks and sectors in both directions.

While we believe that our empirical study has its own value as a contribution to the literature that studies the relation between financial sectors and real sectors, our methodology is quite generally applicable in various contexts of group-wise spillovers, with both directions

of spillover allowed in the same model. Furthermore, our model allows for within group spillover along a network. Such flexibility can be quite useful, for example, in studying peer effects between two groups of students, where each group of students has their own friendship network.

References

ACHARYA, V. V., L. BORCHERT, M. JAGER, AND S. STEFFEN (2021): "Kicking the Can Down the Road: Government Interventions in the European Banking Sector," *The Review of Financial Studies*, 34(9), 4090–4131.

ACHARYA, V. V., M. CROSIGNANI, T. EISERT, AND S. STEFFEN (2022): "Zombie Lending: Theoretical, International and Historical Perspectives," *NBER Working Paper No. 29904*.

ACHARYA, V. V., T. EISERT, C. EUFINGER, AND C. HIRSCH (2019): "Whatever It Takes: The Real Effects of Unconventional Monetary Policy," *The Review of Financial Studies*, 32(9), 3366–3411.

ADALET MCGOWAN, M., D. ANDREWS, AND V. MILLOT (2018): "The Walking Dead? Zombie Firms and Productivity Performance in OECD Countries," *Economic Policy*, 33(96), 685–736.

AHN, S. C., Y. H. LEE, AND P. SCHMIDT (2001): "GMM Estimation of Linear Panel Data Models with Time-Varying Individual Effects," *Journal of Econometrics*, 101, 219–255.

ANDREWS, D., AND F. PETROULAKIS (2019): "Breaking the Shackles: Zombie Firms, Weak Banks and Depressed Restructuring in Europe," *ECB Working Paper No. 2240*.

ARELLANO, M. (2003): "Modeling Optimal Instrumental Variables for Dynamic Panel Data Models," *CEMFI Working Paper No. 0310*.

ARELLANO, M., AND O. BOVER (1995): "Another Look at the Instrumental Variable Estimation of Error-Components Models," *Journal of Econometrics*, 68, 29–51.

ARELLANO, M., AND B. HONORÉ (2001): "Panel Data Models: Some Recent Developments," in *Handbook of Econometrics*, vol. 5, pp. 3229–3296.

BENTOLILA, S., M. JANSEN, AND G. JIMÉNEZ (2018): "When credit dries up: Job losses in the great recession," *Journal of the European Economic Association*, 16(3), 650–695.

BLATTNER, L., L. FARINHA, AND F. REBELO (2019): "When Losses Turn Into Loans: The Cost of Undercapitalized Banks," *ECB Working Paper No. 2228*.

CABALLERO, R. J., T. HOSHI, AND A. K. KASHYAP (2008): "Zombie Lending and Depressed Restructuring in Japan," *American Economic Review*, 98(5), 1943–77.

CHAMBERLAIN, G. (1984): "Panel Data," in *Handbook of Econometrics*, vol. 4, pp. 1247–1318.

CHODOROW-REICH, G. (2014): "The Employment Effects of Credit Market Disruptions: Firm-level Evidence from the 2008–9 Financial Crisis," *The Quarterly Journal of Economics*, 129(1), 1–59.

CHOI, D. (2017): "Estimation of Monotone Treatment Effects in Network Experiments," *Journal of the American Statistical Association*, 112, 1147–1155.

CHOW, Y. S., AND H. TEICHER (1988): *Probability Theory*. Springer-Verlag, Berlin.

DE PAULA, A., I. RASUL, AND P. C. SOUZA (2020): "Identifying Network Ties from Panel Data: Theory and an Application to Tax Competition," *arXiv:1910.07452 [econ.EM]*.

DONALD, S. G., AND W. K. NEWEY (2001): "Choosing the Number of Instruments," *Econometrica*, 69, 1161–1191.

DRUKKER, D. M., P. H. EGGER, AND I. R. PRUCHA (2022): "Simultaneous Equation Models with Higher Order Spatial or Social Network Interactions," *In Press in Econometric Theory*.

DUPREY, T., AND M. LE (2016): "Bankscope Dataset: Getting Started," *SSRN*.

EGAMI, N. (2021): "Spillover Effects in the Presence of Unobserved Networks," *Political Analysis*, 29, 287–316.

FERNANDEZ-VAL, I., AND M. WEIDNER (2018): "Fixed Effects Estimation of Large-T Panel Data Models," *Annual Review of Economics*, 10, 109–138.

FERRANDO, A., A. POPOV, AND G. F. UDELL (2019): "Do SMEs Benefit From Unconventional Monetary Policy and How? Microevidence from the Eurozone," *Journal of Money, Credit and Banking*, 51(4), 895–928.

GARCIA-MACIA, D. (2017): "The Financing of Ideas and the Great Deviation," *IMF Working Paper 17/176*.

GIANNETTI, M., AND S. ONGENA (2012): "Lending by Example: Direct and Indirect Effects of Foreign Banks in Emerging Markets," *Journal of International Economics*, 86(1), 167–180.

GIANNETTI, M., AND A. SIMONOV (2013): "On the Real Effects of Bank Bailouts: Micro Evidence from Japan," *American Economic Journal: Macroeconomics*, 5(1), 135–67.

GOPINATH, G., S. KALEMLI-OZCAN, L. KARABARBOUNIS, AND C. VILLEGAS-SANCHEZ (2017): "Capital Allocation and Productivity in South Europe," *The Quarterly Journal of Economics*, 132(4), 1915–1967.

HAYAKAWA, K. (2009): "A Simple Efficient Instrumental Variable Estimator for Panel AR(p) Models When Both N and T are Large," *Econometric Theory*, 25, 873–890.

HE, X., AND K. SONG (2022): "Measuring Diffusion over a Large Network," *arXiv: 1812.04195v4 [stat.ME]*.

HOLTZ-EAKIN, D., W. NEWEY, AND H. S. ROSEN (1988): "Estimating Vector Autoregressions with Panel Data," *Econometrica*, 56, 1371–1395.

HSIEH, C., AND P. J. KLENOW (2009): "Misallocation and Manufacturing TFP in China and India," *The Quarterly Journal of Economics*, 124(4), 1403–1448.

KALEMLI-OZCAN, S., L. LAEVEN, AND D. MORENO (2022): "Debt Overhang, Rollover Risk, and Corporate Investment: Evidence from the European Crisis," *Journal of the European Economic Association*.

KALEMLI-OZCAN, S., B. SORENSEN, C. VILLEGAS-SANCHEZ, V. VOLOSOVYCH, AND S. YESILTAS (2015): "How to Construct Nationally Representative Firm Level Data from the Orbis Global Database: New Facts and Aggregate Implications," *NBER Working Paper No. 21558*.

KHWAJA, A. I., AND A. MIAN (2008): "Tracing the Impact of Bank Liquidity Shocks: Evidence From an Emerging Market," *American Economic Review*, 98(4), 1413–42.

KOJEVNIKOV, D., V. MARMER, AND K. SONG (2021): "Limit theorems for Network Dependent Random Variables," *Journal of Econometrics*, 222, 882–908.

KOJEVNIKOV, D., AND K. SONG (2021): "Some Impossibility Results with Cluster Dependence with Large Clusters," *arXiv: 21090397v2*.

KUERSTEINER, G. M., AND I. R. PRUCHA (2013): "Limit Theory for Panel Data Models with Cross Sectional Dependence and Sequential Exogeneity," *Journal of econometrics*, 174(2), 107–126.

KUERSTEINER, G. M., AND I. R. PRUCHA (2020): "Dynamic Spatial Panel Models: Networks, Common Shocks, and Sequential Exogeneity," *Econometrica*, 88(5), 2109–2146.

LAEVEN, L., P. MCADAM, AND A. A. POPOV (2018): "Credit Shocks, Employment Protection, and Growth: Firm-level Evidence from Spain," *ECB Working Paper No. 2166*.

LEE, L.-F. (2004): "Asymptotic Distributions of Quasi-Maximum Likelihood Estimators for Spatial Autoregressive Models," *Econometrica*, 72, 1899–1925.

LEE, L.-F., X. LIU, AND X. LIN (2010): "Specification and Estimation of Social Interaction Models with Network Structures," *Econometrics Journal*, 13, 145–176.

LEE, L.-F., AND J. YU (2010): "Some Recent Developments in Spatial Panel Data Models," *Regional Science and Urban Economics*, 40, 255–271.

LEHMANN, E. L., AND J. P. ROMANO (2005): *Testing Statistical Hypotheses*. Springer, New York.

LEUNG, M. P. (2020): "Treatment and Spillover Effects Under Network Interference," 102, 368–380, Review of Economics and Statistics, forthcoming.

LEWBEL, A., X. QU, AND X. TANG (2021): "Social Networks with Unobserved Links," *Working Paper*.

PEEK, J., AND E. S. ROSENGREN (2000): "Collateral Damage: Effects of the Japanese Bank Crisis on Real Activity in the United States," *American Economic Review*, 90(1), 30–45.

——— (2005): "Unnatural Selection: Perverse Incentives and the Misallocation of Credit in Japan," *American Economic Review*, 95(4), 1144–1166.

ROMANO, J. P., AND A. M. SHAIKH (2010): "Inference for the Identified Set in Partially Identified Econometric Models," *Econometrica*, 78, 169–211.

ROMANO, J. P., AND M. WOLF (2005): "Stepwise Multiple Testing as Formalized Data Snooping," *Econometrica*, 73, 1237–1282.

SCHIVARDI, F., E. SETTE, AND G. TABELLINI (2022): "Credit Misallocation During the European Financial Crisis," *The Economic Journal*, 132(641), 391–423.

SCHMIDT, C., Y. SCHNEIDER, S. STEFFEN, AND D. STREITZ (2020): "Capital Misallocation and Innovation," *Working paper*.

SHI, W., AND L.-F. LEE (2017): "Spatial Dynamic Panel Data Models with Interactive Fixed Effects," *Journal of Econometrics*, 197, 323–347.

STORZ, M., M. KOETTER, R. SETZER, AND A. WESTPHAL (2017): "Do We Want These Two to Tango? On Zombie Firms and Stressed Banks in Europe," *ECB Working Paper No. 2104*.

ZHANG, L. (2020): "Spillovers of Program Benefits with Mismeasured Networks," *Working Paper*.

SUPPLEMENTAL NOTE TO "ESTIMATING DYNAMIC SPILLOVER EFFECTS ALONG MULTIPLE NETWORKS IN A LINEAR PANEL MODEL"

Clemens Possnig[22], Andreea Rotărescu[23], and Kyungchul Song[24]

This Online Appendix consists of three sections. The first section provides the mathematical proofs of the results in the main paper. The second section gives more results from our Monte Carlo simulation study. The third section gives details on further results from the empirical study of bank-sector spillover in Spain.

1. Mathematical Proofs

In this section, we provide mathematical proofs of Theorems 3.1-3.2. Throughout the appendix, we assume that Assumptions 3.1-3.5 hold. The following representation shows the advantage of the Helmert transform: the error term $\hat{U}_K$ after the transform can be written as a sum of martingale difference arrays with filtrations $\{\mathcal{F}_s\}_{s=1}^T$.

Lemma 1.1. *For $K \in \{B, F\}$,*

$$\sqrt{n_K}\hat{U}_K = \sum_{s=1}^{T} \xi^*_{s,K} + o_P(1),$$

where $\xi^*_{s,K}$ is defined in (3.8).

Proof: Let

$$\varepsilon^G_{i,s} = \frac{1}{|N_G(i)|} \sum_{i \in N_G(i)} \varepsilon_{i,t}, \text{ and } \nu^G_i = \frac{1}{|N_G(i)|} \sum_{i \in N_G(i)} \nu_i. \tag{1.1}$$

[22]Vancouver School of Economics, University of British Columbia
[23]Department of Economics, Johns Hopkins University
[24]Vancouver School of Economics, University of British Columbia

We write

$$\begin{aligned}\sqrt{n_K}\hat{U}_K = \sqrt{n_K}\sum_{t=1}^{T-1}\hat{U}_{t,K} &= \frac{1}{\sqrt{n_K}}\sum_{t=1}^{T-1}\sum_{s=t}^{T}h_{s,t}\sum_{i\in N_K}(Z_{i,t}-Z_{i,t}^G)(u_{i,s}-u_{i,s}^G)\\ &= \frac{1}{\sqrt{n_K}}\sum_{t=1}^{T-1}\sum_{s=t}^{T}h_{s,t}\sum_{i\in N_K}(Z_{i,t}-Z_{i,t}^G)(\varepsilon_{i,s}+\nu_i-(\varepsilon_{i,s}^G+\nu_i^G))\\ &= \frac{1}{\sqrt{n_K}}\sum_{t=1}^{T-1}\sum_{s=t}^{T}h_{s,t}\sum_{i\in N_K}(Z_{i,t}-Z_{i,t}^G)(\varepsilon_{i,s}+\nu_i).\end{aligned}$$

The last equality follows due to the mean deviation $Z_{i,t}-Z_{i,t}^G$. By the definition of $h_{s,t}$, we have $\sum_{s=t}^{T}h_{s,t}=0$, and hence the last sum is equal to

$$\frac{1}{\sqrt{n_K}}\sum_{i\in N_K}\sum_{t=1}^{T-1}(Z_{i,t}-Z_{i,t}^G)\sum_{s=t}^{T}h_{s,t}\varepsilon_{i,s} = \sum_{s=1}^{T}\frac{1}{\sqrt{n_K}}\sum_{i\in N_K}\sum_{t=1}^{s\wedge(T-1)}h_{s,t}(Z_{i,t}-Z_{i,t}^G)\varepsilon_{i,s}.$$

Now, by Assumption 3.2, we have

$$\begin{aligned}(1.2)\quad \mathbf{E}\left[\left\|\frac{1}{\sqrt{n_K}}\sum_{i\in N_K}(Z_{i,t}-Z_{i,t}^*)\varepsilon_{i,s}\right\|^2 \mid \mathcal{F}_s\right] &= \frac{1}{n_K}\sum_{i\in N_K}\left\|Z_{i,t}-Z_{i,t}^*\right\|^2\mathbf{E}\left[\varepsilon_{i,s}^2\mid\mathcal{F}_s\right]\\ &\le \max_{i\in N}\mathbf{E}\left[\varepsilon_{i,s}^2\mid\mathcal{F}_s\right]\frac{1}{n_K}\sum_{i\in N_K}\left\|Z_{i,t}-Z_{i,t}^*\right\|^2 = o_P(1),\end{aligned}$$

and

$$\sqrt{n_K}\hat{U}_K = \sum_{s=1}^{T}\frac{1}{\sqrt{n_K}}\sum_{i\in N_K}\sum_{t=1}^{s\wedge(T-1)}h_{s,t}(Z_{i,t}^*-Z_{i,t}^{*G})\varepsilon_{i,s}+o_P(1).$$

■

Recall the definition: for $K\in\{B,F\}$,

$$N_{t,\ell,K}(i)=\{j\in N_K : j\in N_{t,\ell}(i)\}.$$

For each $t=1,\dots,T-1$ and $i\in N$, define

$$N_t(i)=\left\{j\in N : j\in N_{t,\ell,K}(i),\ \text{for some } \ell=1,\dots,L,\ \text{and some } K\in\{B,F\}\right\},$$

and $\overline{N}_t(i)=N_t(i)\cup\{i\}$. Thus $N_t(i)$ represents the union of the in-neighborhoods $N_{t,\ell,K}(i)$, $\ell=1,\dots,L$ and $K\in\{B,F\}$.

Lemma 1.2. *For $K\in\{B,F\}$, as $n_K\to\infty$,*

$$\frac{1}{n_K}\sum_{i\in N_K}\left(\tilde{Z}_{i,s}W_{i,s}^\top-\mathbf{E}\left[\tilde{Z}_{i,s}^*W_{i,s}^\top\mid\mathcal{F}_{s-1}\right]\right)\to_p 0.$$

Proof: By Assumption 3.2, it is not hard to see that

$$\frac{1}{n_K}\sum_{i\in N_K}\left(\tilde{Z}_{i,s}-\tilde{Z}^*_{i,s}\right)W_{i,s}^\top = o_P(1).$$

For $k=1,...,d_Z$ and $m=1,...,d_W$, we let $\tilde{Z}^*_{i,s,k}$ be the k-th entry of $\tilde{Z}^*_{i,s}$ and $W_{i,s,m}$ be the m-th entry of $W_{i,s,m}$. For any such k,m, once we condition on $\mathcal{F}_{s-1}$, the randomness of $\tilde{Z}^*_{i,s,k}W_{i,s,m}$ solely comes from $(\varepsilon_{j,s-1})_{j\in\overline{N}_s(i)}$. Furthermore, $\overline{N}_s(i)$ is already $\mathcal{F}_{s-1}$-measurable. By Assumptions 3.1(i) and (ii), we have

$$\mathrm{Cov}\left(\tilde{Z}^*_{i,s,k}W_{i,s,m},\tilde{Z}^*_{j,s,k}W_{j,s,m}\mid\mathcal{F}_{s-1}\right)=0,$$

whenever $\overline{N}_s(i)\cap\overline{N}_s(j)=\varnothing$. Therefore,

$$\mathrm{Var}\left(\frac{1}{n_K}\sum_{i\in N_K}\tilde{Z}^*_{i,s,k}W_{i,s,m}\mid\mathcal{F}_{s-1}\right)=\frac{1}{n_K^2}\sum_{i,j\in N:\overline{N}_s(i)\cap\overline{N}_s(j)\neq\varnothing}\mathrm{Cov}\left(\tilde{Z}^*_{i,s,k}W_{i,s,m},\tilde{Z}^*_{j,s,k}W_{j,s,m}\mid\mathcal{F}_{s-1}\right).$$

By Assumptions 3.3 and 3.5, we find that the last term is $o_P(1)$. ■

Lemma 1.3. *For each $K\in\{B,F\}$, as $n_K\to\infty$, $\hat{B}_K-B_{n,K}\to_P 0$, where $\hat{B}_K$ and $B_{n,K}$ are defined in (3.3) and (3.9).*

Proof: First we write

$$\sum_{t=1}^{T-1}\frac{1}{n_K}\sum_{i\in N_K}\left(Z_{i,t}-Z^G_{i,t}\right)W^{H\top}_{i,t}=\sum_{s=1}^{T}\frac{1}{n_K}\sum_{i\in N_K}\tilde{Z}_{i,s}\left(W_{i,s}-W^G_{i,s}\right)^\top=\sum_{s=1}^{T}\frac{1}{n_K}\sum_{i\in N_K}\tilde{Z}_{i,s}W_{i,s}^\top.$$

Then we write that for each $s=1,...,T$,

$$\frac{1}{n_K}\sum_{i\in N_K}\tilde{Z}_{i,s}W_{i,s}^\top=\frac{1}{n_K}\sum_{i\in N_K}\mathbf{E}\left[\tilde{Z}^*_{i,s}W_{i,s}^\top\mid\mathcal{F}_{s-1}\right]+o_P(1),$$

by Lemma 1.2. This gives the desired result. ■

Lemma 1.4. *For $K\in\{B,F\}$, as $n_K\to\infty$, $\tilde{\delta}_K-\delta_K=o_P(1)$.*

Proof: We first show that $\hat{U}_K=o_P(1)$. Recall that by construction $u^H_{i,t}=\varepsilon^H_{i,t}$ holds for all i,t. We can then write

$$\hat{U}_K=\sum_{t=1}^{T-1}\frac{1}{n_K}\sum_{i\in N_K}(Z_{i,t}-Z^G_{i,t})u^H_{i,t}=\sum_{s=1}^{T}\frac{1}{n_K}\sum_{i\in N_K}\tilde{Z}_{i,s}(\varepsilon_{i,s}-\varepsilon^G_{i,s})=\sum_{s=1}^{T}\frac{1}{n_K}\sum_{i\in N_K}\tilde{Z}_{i,s}\varepsilon_{i,s}.$$

The last equality comes from the fact that $\tilde{Z}_{i,s}$ is a mean-deviated form. Hence we can write

$$\hat{U}_K=\frac{1}{\sqrt{n_K}}\sum_{s=1}^{T}\xi_{s,K}=\frac{1}{\sqrt{n_K}}\sum_{s=1}^{T}\xi^*_{s,K}+o_P(1).$$

Note that

$$\sum_{s=1}^{T}\text{Var}(\xi^*_{s,K}\mid\mathcal{F}_s)=\sum_{s=1}^{T}\frac{1}{n_K}\sum_{i\in N_K}\sigma^2_{n,\varepsilon,s}\tilde{Z}^*_{i,s}\tilde{Z}^{*\top}_{i,s}$$
$$=\sum_{s=1}^{T}\frac{1}{n_K}\sum_{i\in N_K}\sigma^2_{\varepsilon,s}\tilde{Z}^*_{i,s}\tilde{Z}^{*\top}_{i,s}+o_P(1)$$
$$=\sum_{s=1}^{T}\frac{1}{n_K}\sum_{i\in N_K}\sigma^2_{\varepsilon,s}\mathbf{E}\left[\tilde{Z}^*_{i,s}\tilde{Z}^{*\top}_{i,s}\mid\mathcal{F}_{s-1}\right]+o_P(1)=\Omega_K+o_P(1),$$

by following the same arguments as in the proof of Lemma 1.2 and Assumption 3.4. Choose any $\epsilon>0$ and let $M^2_\epsilon>0$ be a large number such that

$$P\left\{\mathbf{E}[\|\xi^*_{s,K}\|^2\mid\mathcal{F}_s]>M^2_\epsilon\right\}<\epsilon. \tag{1.3}$$

Define $1_s=1\{\mathbf{E}[\|\xi^*_{s,K}\|^2\mid\mathcal{F}_s]\leq M^2_\epsilon\}$. For each $s=1,...,T$, and any $\epsilon>0$,

$$P\left\{\|\xi^*_{s,K}\|^2>M^2_\epsilon\right\}\leq\frac{\mathbf{E}\left[M^2_\epsilon 1_s+\mathbf{E}[\|\xi^*_{s,K}\|^2\mid\mathcal{F}_s](1-1_s)\right]}{M^4_\epsilon}$$
$$\leq\frac{1}{M^2_\epsilon}+\frac{\epsilon^{1/2}\sqrt{\mathbf{E}\left[\left(\mathbf{E}[\|\xi^*_{s,K}\|^2\mid\mathcal{F}_s]\right)^2\right]}}{M^4_\epsilon},$$

using Cauchy-Schwarz inequality and (1.3). The left hand side made arbitrarily small by choosing large enough M_ϵ and Assumption 3.5. Hence, for $K\in\{B,F\}$, $\xi^*_{s,K}=O_P(1)$, as $n_K\to\infty$. We conclude that $\hat{U}_K=O_P(n_K^{-1/2})=o_P(1)$. Hence

$$\tilde{\delta}_K-\delta_K=\left(\hat{B}^\top_K\hat{B}_K\right)^{-1}\hat{B}^\top_K\hat{U}_K=\left(B^\top_K B_K\right)^{-1}B^\top_K\hat{U}_K+o_P(1)=o_P(1), \tag{1.4}$$

by Lemma 1.3 and Assumption 3.4. ■

For $K\in\{B,F\}$, we recall the definition of $\Omega^\circ_{n,s,K}$ in (3.9). We define

$$\Omega_{n,K}=\sum_{s=1}^{T}\Omega^\circ_{n,s,K}. \tag{1.5}$$

Lemma 1.5. *For $K\in\{B,F\}$, as $n_K\to\infty$, $\hat{\Omega}_K-\Omega_{n,K}\to_p 0$.*

Proof: Since $\hat{u}^H_{i,t,K}-u^H_{i,t}=W^{H\top}_{i,t}(\delta_K-\tilde{\delta}_K)$, we write

$$\hat{\Omega}_K=\sum_{t=1}^{T-1}\sum_{t'=1}^{T-1}\frac{1}{n_K}\sum_{i\in N_K}\left(Z_{i,t}-Z^G_{i,t}\right)\left(Z_{i,t'}-Z^G_{i,t'}\right)^\top\hat{u}^H_{i,t,K}\hat{u}^H_{i,t',K}$$
$$=\sum_{t=1}^{T-1}\sum_{t'=1}^{T-1}\frac{1}{n_K}\sum_{i\in N_K}\left(Z_{i,t}-Z^G_{i,t}\right)\left(Z_{i,t'}-Z^G_{i,t'}\right)^\top u^H_{i,t}u^H_{i,t'}+R_n,$$

where

$$R_n = \sum_{t=1}^{T-1}\sum_{t'=1}^{T-1}\sum_{k=1}^{d_W}\sum_{k'=1}^{d_W}(\delta_{0,k}-\tilde{\delta}_k)\left(\frac{1}{n_K}\sum_{i\in N_K} W^H_{i,t,k}\left(Z_{i,t}-Z^G_{i,t}\right)\left(Z_{i,t'}-Z^G_{i,t'}\right)^\top W^H_{i,t',k'}\right)(\delta_{0,k'}-\tilde{\delta}_{k'}),$$

with $W^H_{i,t,k}$ denoting the k-th entry of $W^H_{i,t}$ and similarly with $\delta_{0,k}$ and $\tilde{\delta}_k$. Note that

$$\begin{aligned}
&\sum_{t=1}^{T-1}\sum_{t'=1}^{T-1}\frac{1}{n_K}\sum_{i\in N_K} W^H_{i,t,k}\left(Z_{i,t}-Z^G_{i,t}\right)\left(Z_{i,t'}-Z^G_{i,t'}\right)^\top W^H_{i,t',k'}\\
&=\sum_{s=1}^{T}\sum_{s'=1}^{T}\frac{1}{n_K}\sum_{i\in N_K} W_{i,s,k}\tilde{Z}_{i,s}\tilde{Z}^\top_{i,s'}W_{i,s',k'}\\
&=\frac{1}{n_K}\sum_{i\in N_K}\left(\sum_{s=1}^{T}W_{i,s,k}\tilde{Z}_{i,s}\right)\left(\sum_{s=1}^{T}W_{i,s,k'}\tilde{Z}_{i,s}\right)^\top.
\end{aligned}$$

By Cauchy-Schwarz inequality, we bound the (m,m')-th entry of the last term by

$$\sqrt{\frac{1}{n_K}\sum_{i\in N_K}\left(\sum_{s=1}^{T}W_{i,s,k}\tilde{Z}_{i,s,m}\right)^2}\times\sqrt{\frac{1}{n_K}\sum_{i\in N_K}\left(\sum_{s=1}^{T}W_{i,s,k}\tilde{Z}_{i,s,m'}\right)^2},$$

where $\tilde{Z}_{i,s,m}$ denotes the m-th entry of $\tilde{Z}_{i,s}$. We write

$$\begin{aligned}
\frac{1}{n_K}\sum_{i\in N_K}\left(\sum_{s=1}^{T}W_{i,s,k}\tilde{Z}_{i,s,m}\right)^2 &= \sum_{s=1}^{T}\sum_{s'=1}^{T}\frac{1}{n_K}\sum_{i\in N_K}W_{i,s,k}W_{i,s',k}\tilde{Z}_{i,s,m}\tilde{Z}_{i,s',m}\\
&\le \sum_{s=1}^{T}\sum_{s'=1}^{T}\sqrt{\frac{1}{n_K}\sum_{i\in N_K}\tilde{Z}^2_{i,s,m}W^2_{i,s,k}}\sqrt{\frac{1}{n_K}\sum_{i\in N_K}\tilde{Z}^2_{i,s',m}W^2_{i,s',k}}.
\end{aligned}$$

Using the same arguments as in the proof of Lemma 1.2,

$$\begin{aligned}
\frac{1}{n_K}\sum_{i\in N_K}\tilde{Z}^2_{i,s,m}W^2_{i,s,k} &= \frac{1}{n_K}\sum_{i\in N_K}\mathbf{E}\left[\tilde{Z}^{*2}_{i,s,m}W^2_{i,s,k}\mid\mathcal{F}_{s-1}\right]+o_P(1)\\
&\le \sqrt{\frac{1}{n_K}\sum_{i\in N_K}\mathbf{E}\left[\|W_{i,s}\|^4\mid\mathcal{F}_{s-1}\right]}\times\sqrt{\frac{1}{n_K}\sum_{i\in N_K}\mathbf{E}\left[\|\tilde{Z}^*_{i,s}\|^4\mid\mathcal{F}_{s-1}\right]}+o_P(1).
\end{aligned}$$

By Assumptions 3.2 and 3.5, we find that

$$\frac{1}{n_K}\sum_{i\in N_K} W^H_{i,t,k}\left(Z_{i,t}-Z^G_{i,t}\right)\left(Z_{i,t'}-Z^G_{i,t'}\right)^\top W^H_{i,t',k'} = O_P(1).$$

Since $\tilde{\delta}_K = \delta_K + o_P(1)$ by Lemma 1.4, we have

$$\begin{aligned}
&\frac{1}{n_K}\sum_{i\in N_K}\left(Z_{i,t}-Z^G_{i,t}\right)\left(Z_{i,s}-Z^G_{i,s}\right)^\top \hat{u}^H_{i,t,K}\hat{u}^H_{i,s,K}\\
&=\frac{1}{n_K}\sum_{i\in N_K}\left(Z_{i,t}-Z^G_{i,t}\right)\left(Z_{i,s}-Z^G_{i,s}\right)^\top u^H_{i,t}u^H_{i,s}+o_P(1).
\end{aligned}$$

This gives us

$$\begin{aligned}
\hat{\Omega}_K &= \frac{1}{n_K}\sum_{i\in N_K}\left(\sum_{t=1}^{T-1}\left(Z_{i,t}-Z^G_{i,t}\right)u^H_{i,t}\right)\left(\sum_{t=1}^{T-1}\left(Z_{i,t}-Z^G_{i,t}\right)u^H_{i,t}\right)^\top + o_P(1)\\
&= \frac{1}{n_K}\sum_{i\in N_K}\left(\sum_{s=1}^{T}\tilde{Z}_{i,s}\varepsilon_{i,s}\right)\left(\sum_{s=1}^{T}\tilde{Z}_{i,s}\varepsilon_{i,s}\right)^\top + o_P(1)\\
&= \frac{1}{n_K}\sum_{i\in N_K}\left(\sum_{s=1}^{T}\tilde{Z}^*_{i,s}\varepsilon_{i,s}\right)\left(\sum_{s=1}^{T}\tilde{Z}^*_{i,s}\varepsilon_{i,s}\right)^\top + o_P(1).
\end{aligned}$$

where the second equality is due to our derivation above, and the third equality due to (1.2).

For $s \neq s'$, we have

$$\mathbf{E}\left[\left(\tilde{Z}^*_{i,s,k}\tilde{Z}^*_{i,s',k'}\right)\varepsilon_{i,s}\varepsilon_{i,s'} \mid \mathcal{F}_0\right] = 0.$$

Hence

$$\begin{aligned}
&\mathrm{Var}\left(\frac{1}{n_K}\sum_{i\in N_K}\tilde{Z}^*_{i,s,k}\tilde{Z}^*_{i,s',k'}\varepsilon_{i,s}\varepsilon_{i,s'} \mid \mathcal{F}_0\right)\\
&= \frac{1}{n_K^2}\sum_{i\in N_K}\mathbf{E}\left[\left(\tilde{Z}^*_{i,s,k}\tilde{Z}^*_{i,s,k'}\right)^2\varepsilon^2_{i,s}\varepsilon^2_{i,s'} \mid \mathcal{F}_0\right]\\
&\leq \frac{1}{n_K}\sqrt{\frac{1}{n_K}\sum_{i\in N_K}\mathbf{E}\left[\left(\tilde{Z}^*_{i,s,k}\varepsilon_{i,s}\right)^4 \mid \mathcal{F}_0\right]}\sqrt{\frac{1}{n_K}\sum_{i\in N_K}\mathbf{E}\left[\left(\tilde{Z}^*_{i,s,k'}\varepsilon_{i,s}\right)^4 \mid \mathcal{F}_0\right]}.
\end{aligned}$$

Since

$$\frac{1}{n_K}\sum_{i\in N_K}\mathbf{E}\left[\tilde{Z}^{*4}_{i,s,k}\varepsilon^4_{i,s} \mid \mathcal{F}_s\right] \leq \frac{1}{n_K}\sum_{i\in N_K}\tilde{Z}^{*4}_{i,s,k}\max_{i\in N}\mathbf{E}\left[\varepsilon^4_{i,s} \mid \mathcal{F}_s\right] = O_P(1),$$

we find that whenever $s \neq s'$,

$$\mathrm{Var}\left(\frac{1}{n_K}\sum_{i\in N_K}\tilde{Z}^*_{i,s,k}\tilde{Z}^*_{i,s',k'}\varepsilon_{i,s}\varepsilon_{i,s'} \mid \mathcal{F}_0\right) = O_P(n_K^{-1}).$$

Hence

$$\begin{aligned}\hat{\Omega}_K &= \frac{1}{n_K}\sum_{i\in N_K}\sum_{s=1}^{T}\tilde{Z}^*_{i,s}\tilde{Z}^{*\top}_{i,s}\varepsilon^2_{i,s} + o_P(1)\\ &= \frac{1}{n_K}\sum_{i\in N_K}\sum_{s=1}^{T}\tilde{Z}^*_{i,s}\tilde{Z}^{*\top}_{i,s}\sigma^2_{\varepsilon,s} + o_P(1)\\ &= \frac{1}{n_K}\sum_{i\in N_K}\sum_{s=1}^{T}\sigma^2_{\varepsilon,s}\mathbf{E}\left[\tilde{Z}^*_{i,s}\tilde{Z}^{*\top}_{i,s} \mid \mathcal{F}_{s-1}\right] + o_P(1) = \Omega_{n,K} + o_P(1).\end{aligned}$$

■

For each $s = 1, .., T$, let $\xi^*_s = [\xi^{*\top}_{s,B}, \xi^{*\top}_{s,F}]^\top$, and

$$\tilde{\Omega}^\circ_{n,s} = \mathrm{Var}\left(\xi^*_s \mid \mathcal{F}_s\right). \tag{1.6}$$

We can write

$$\xi^*_s = \frac{1}{\sqrt{n}}\sum_{i\in N}\Lambda_{i,s}\varepsilon_{i,s},$$

where $\Lambda_{i,s} = [\tilde{Z}^{*\top}_{i,s}1_{i,B}, \tilde{Z}^{*\top}_{i,s}1_{i,F}]^\top$, and

$$1_{i,B} = \frac{1\{i\in N_B\}\sqrt{n}}{\sqrt{n_B}}, \text{ and } 1_{i,F} = \frac{1\{i\in N_F\}\sqrt{n}}{\sqrt{n_F}}.$$

After some algebra, it is not hard to see that for each $s = 1, ..., T$,

$$\tilde{\Omega}^\circ_{n,s} = \begin{bmatrix} \frac{\sigma^2_{n,\varepsilon,s}}{n_B}\sum_{i\in N_B}\tilde{Z}^*_{i,s}\tilde{Z}^{*\top}_{i,s} & 0 \\ 0 & \frac{\sigma^2_{n,\varepsilon,s}}{n_F}\sum_{i\in N_F}\tilde{Z}^*_{i,s}\tilde{Z}^{*\top}_{i,s}\end{bmatrix}. \tag{1.7}$$

Lemma 1.6. *For any vector $b \in \mathbf{R}^{2d_Z}$ such that $b^\top b = 1$, and for each $s = 1, ..., T$,*

$$\sup_{\tilde{c}\in\mathbf{R}}\left|P\left\{b^\top\xi^*_s \le \tilde{c} \mid \mathcal{F}_s\right\} - P\left\{b^\top\tilde{\xi}_s \le \tilde{c} \mid \mathcal{F}_s\right\}\right| \le \frac{7.5}{\sqrt{n}}\frac{\frac{1}{n}\sum_{i\in N}|b^\top\Lambda_{i,s}|^3\mathbf{E}\left[|\varepsilon_{i,s}|^3 \mid \mathcal{F}_s\right]}{\left(b^\top\left(\frac{1}{n}\sum_{i\in N}\Lambda_{i,s}\Lambda^\top_{i,s}\sigma^2_{n,\varepsilon,s}\right)b\right)^{3/2}},$$

where $\tilde{\xi}_s = (\tilde{\Omega}^\circ_{n,s})^{1/2}\mathbb{Z}$, $\mathbb{Z} \in \mathbf{R}^{2d_Z}$ is a random vector following $N(0, I)$ and independent of all other random variables and $\tilde{\Omega}^\circ_{n,s}$ is defined in (1.6).

Proof: Since $\varepsilon_{i,s}$, $i = 1, ..., n$, are conditionally independent given $\mathcal{F}_s$, we use the Berry-Esseen bound (Theorem 3 of Chow and Teicher (1988), p.304).[25] ■

Lemma 1.7. *For any vector $b \in \mathbf{R}^{2d_Z}$ such that $b^\top b = 1$ and for $\tilde{c} \in \mathbf{R}$,*

$$P\left\{\sum_{s=1}^{T} b^\top \xi_s^* \leq \tilde{c} \mid \mathcal{F}_0\right\} - P\left\{\sum_{s=1}^{T} b^\top \tilde{\xi}_s \leq \tilde{c} \mid \mathcal{F}_0\right\} = \sum_{s=1}^{T} \mathbf{E}\left[\Delta_{s-1}\left(\tilde{c} - b^\top R_s\right) \mid \mathcal{F}_0\right],$$

where

$$\begin{aligned}\Delta_{s-1}\left(\tilde{c} - b^\top R_s\right) = P&\left\{b^\top \xi_s^* \leq \tilde{c} - \sum_{t=s+1}^{T} b^\top \tilde{\xi}_t - b^\top R_{s-1} \mid \mathcal{F}_s\right\} \\ &- P\left\{b^\top \tilde{\xi}_s \leq \tilde{c} - \sum_{t=s+1}^{T} b^\top \tilde{\xi}_t - b^\top R_{s-1} \mid \mathcal{F}_s\right\}\end{aligned}$$

and $R_s = \sum_{t=1}^{s} \xi_t^*$, $R_0 = 0$, and $\tilde{\xi}_s$, with $s = 1, ..., T$, are defined in Lemma 1.6.

Proof: First, we write

$$\begin{aligned}P\left\{\sum_{s=1}^{T} b^\top \xi_s^* \leq \tilde{c} \mid \mathcal{F}_T\right\} &= P\left\{b^\top \xi_T^* \leq \tilde{c} - b^\top R_{T-1} \mid \mathcal{F}_T\right\} \\ &= P\left\{b^\top \tilde{\xi}_T \leq \tilde{c} - b^\top R_{T-1} \mid \mathcal{F}_T\right\} + \Delta_{T-1}(\tilde{c} - b^\top R_{T-1}),\end{aligned}$$

where

$$\begin{aligned}\Delta_{T-1}(\tilde{c} - b^\top R_{T-1}) = P&\left\{b^\top \xi_T^* \leq \tilde{c} - b^\top R_{T-1} \mid \mathcal{F}_T\right\} \\ &- P\left\{b^\top \tilde{\xi}_T \leq \tilde{c} - b^\top R_{T-1} \mid \mathcal{F}_T\right\}.\end{aligned}$$

We write

$$\begin{aligned}P\left\{b^\top \tilde{\xi}_T \leq \tilde{c} - b^\top R_{T-1} \mid \mathcal{F}_{T-1}\right\} &= P\left\{b^\top \xi_{T-1}^* \leq \tilde{c} - b^\top \tilde{\xi}_T - b^\top R_{T-2} \mid \mathcal{F}_{T-1}\right\} \\ &= P\left\{b^\top \tilde{\xi}_{T-1} + b^\top \tilde{\xi}_T \leq \tilde{c} - b^\top R_{T-2} \mid \mathcal{F}_{T-1}\right\} \\ &\quad + \Delta_{T-1}(\tilde{c} - b^\top R_{T-2}).\end{aligned}$$

We continue this procedure until we have

$$\begin{aligned}&P\left\{b^\top \tilde{\xi}_2 \leq \tilde{c} - b^\top \tilde{\xi}_T - b^\top \tilde{\xi}_{T-1} \cdots - b^\top \tilde{\xi}_3 - b^\top R_1 \mid \mathcal{F}_1\right\} \\ &= P\left\{b^\top \xi_1^* \leq \tilde{c} - b^\top \tilde{\xi}_T - b^\top \tilde{\xi}_{T-1} \cdots - b^\top \tilde{\xi}_2 \mid \mathcal{F}_1\right\} \\ &= P\left\{b^\top \tilde{\xi}_T + b^\top \tilde{\xi}_{T-1} \cdots + b^\top \tilde{\xi}_2 + b^\top \tilde{\xi}_1 \leq \tilde{c} \mid \mathcal{F}_1\right\} + \Delta_0(c - b^\top R_0),\end{aligned}$$

[25] The theorem itself is concerned with the sum of independent random variables. However, with appropriate modifications, the same bound with replacing the moments by the conditional moments given the common shock applies to a sum of conditionally independent random variables given the common shocks.

where $R_0 = 0$, and

$$\begin{aligned}\Delta_0(c - b^\top R_0) = P\left\{b^\top \xi_1^* \le \tilde{c} - b^\top \tilde{\xi}_T - b^\top \tilde{\xi}_{T-1} \cdots - b^\top \tilde{\xi}_2 \mid \mathcal{F}_1\right\} \\ - P\left\{b^\top \tilde{\xi}_1 \le \tilde{c} - b^\top \tilde{\xi}_T - b^\top \tilde{\xi}_{T-1} \cdots - b^\top \tilde{\xi}_2 \mid \mathcal{F}_1\right\}.\end{aligned}$$

By taking conditional expectations given $\mathcal{F}_0$ of all the conditional probabilities above, we obtain the desired result. ■

Define

$$\hat{U} = \frac{1}{\sqrt{n}} \sum_{s=1}^{T} \xi_s^*. \tag{1.8}$$

For $K \in \{B, F\}$, let $\Omega_K = \sum_{s=1}^{T} \Omega_{s,K}^\circ$, with $\Omega_{s,K}^\circ$ being the matrix in Assumption 3.4. Let

$$\Omega = \begin{bmatrix} \Omega_B & 0 \\ 0 & \Omega_F \end{bmatrix}, \text{ and } \Omega_{n,s}^\circ = \begin{bmatrix} \Omega_{n,s,B}^\circ & 0 \\ 0 & \Omega_{n,s,F}^\circ \end{bmatrix},$$

where $\Omega_{n,s,K}^\circ$ is the matrix defined in (3.9).

Lemma 1.8. *As $n \to \infty$, for any vector $b \in \mathbf{R}^{2d_Z}$ such that $b^\top b = 1$,*

$$\sup_{\tilde{c} \in \mathbf{R}} \left| P\left\{\sqrt{n} b^\top \hat{U} \le \tilde{c} \mid \mathcal{F}_0\right\} - P\left\{b^\top \Omega^{1/2} \mathbb{Z} \le \tilde{c} \mid \mathcal{F}_0\right\} \right| \to_P 0,$$

where $\mathbb{Z} \in \mathbf{R}^{2dZ}$ is a standard normal random vector.

Proof: Note that for each $s = 1, ..., T$,

$$\begin{aligned}\frac{1}{n} \sum_{i \in N} \sigma_{n,\varepsilon,s}^2 \Lambda_{i,s} \Lambda_{i,s}^\top &= \frac{1}{n} \sum_{i \in N} \sigma_{n,\varepsilon,s}^2 \mathbf{E}\left[\Lambda_{i,s} \Lambda_{i,s}^\top \mid \mathcal{F}_{s-1}\right] + o_P(1) \\ &= \Omega_{n,s}^\circ \to \Omega, \text{ as } n \to \infty.\end{aligned}$$

Furthermore,

$$\begin{aligned}\frac{1}{n} \sum_{i \in N} |b^\top \Lambda_{i,s}|^3 \mathbf{E}\left[|\varepsilon_{i,s}|^3 \mid \mathcal{F}_s\right] &\le \max_{i \in N} \mathbf{E}\left[|\varepsilon_{i,s}|^3 \mid \mathcal{F}_s\right] \frac{1}{n} \sum_{i \in N} |b^\top \Lambda_{i,s}|^3 \\ &= O_P(1) \times \frac{1}{n} \sum_{i \in N} \mathbf{E}\left[|b^\top \Lambda_{i,s}|^3 \mid \mathcal{F}_{s-1}\right] + o_P(1) = O_P(1),\end{aligned}$$

by the same arguments in the proof of Lemma 1.2 and Assumption 3.4. Hence we have the bound in Lemma 1.6 as

$$\frac{7.5}{\sqrt{n}} \frac{\frac{1}{n} \sum_{i \in N} |b^\top \Lambda_{i,s}|^3 \mathbf{E}\left[|\varepsilon_{i,s}|^3 \mid \mathcal{F}_s\right]}{\left(b^\top \left(\frac{1}{n} \sum_{i \in N} \sigma_{n,\varepsilon,s}^2 \Lambda_{i,s} \Lambda_{i,s}^\top\right) b\right)^{3/2}} = O_P(n^{-1/2}).$$

Therefore, by Lemma 1.7,

$$\sup_{\tilde{c}\in\mathbf{R}}\left|P\left\{\sum_{s=1}^{T}b^{\top}\xi_{s}^{*}\leq\tilde{c}\mid\mathcal{F}_{0}\right\}-P\left\{\sum_{s=1}^{T}b^{\top}\tilde{\xi}_{s}\leq\tilde{c}\mid\mathcal{F}_{0}\right\}\right|\rightarrow_{p}0,$$

as $n\rightarrow\infty$. We write

$$P\left\{\sum_{s=1}^{T}b^{\top}\tilde{\xi}_{s}\leq\tilde{c}\mid\mathcal{F}_{T}\right\}=P\left\{\sum_{s=1}^{T}b^{\top}(\tilde{\Omega}_{n,s}^{\circ})^{1/2}\mathbb{Z}_{s}\leq\tilde{c}\mid\mathcal{F}_{T}\right\}+o_{p}(1), \tag{1.9}$$

where $\tilde{\Omega}_{n,s}^{\circ}$ is defined in (1.6) and expressed as in (1.7). Using the same arguments in the proof of Lemma 1.2, we find that as $n\rightarrow\infty$, $\tilde{\Omega}_{n,s}^{\circ}=\Omega_{n,s}^{\circ}+o_{p}(1)$, by Assumption 3.4. Hence the probability on the right hand side of (1.9) is equal to

$$P\left\{\sum_{s=1}^{T}b^{\top}(\Omega_{n,s}^{\circ})^{1/2}\mathbb{Z}_{s}\leq\tilde{c}\mid\mathcal{F}_{T}\right\}+o_{p}(1).$$

Since $\mathbb{Z}_{s}$ are independent across s and all independent of $\mathcal{F}_{T}$ and $\Omega_{n,s}^{\circ}$ is $\mathcal{F}_{T}$-measurable, the conditional distribution of $\sum_{s=1}^{T}b^{\top}(\Omega_{n,s}^{\circ})^{1/2}\mathbb{Z}_{s}$ given $\mathcal{F}_{T}$ is Gaussian with mean zero and its variance is equal to $b^{\top}(\sum_{s=1}^{T}\Omega_{n,s}^{\circ})b$. By Assumption 3.4, $\sum_{s=1}^{T}\Omega_{n,s}^{\circ}=\Omega+o_{p}(1)$, and the matrix Ω is $\mathcal{F}_{0}$ measurable. Hence the conditional probability on the right hand side of (1.9) equals

$$P\left\{b^{\top}\Omega^{1/2}\mathbb{Z}_{1}\leq\tilde{c}\mid\mathcal{F}_{T}\right\}+o_{p}(1).$$

By taking a conditional expectation on $\mathcal{F}_{0}$ and using the law of iterated conditional expectations and the bounded convergence theorem (for convergence in measure), we obtain the desired result. ■

Proof of Theorem 3.1: From the definition of $\hat{U}$ in (1.8), we write

$$\sqrt{n}\hat{U}=\sum_{s=1}^{T}\begin{bmatrix}\frac{1}{\sqrt{n}}\sum_{i\in N}\tilde{Z}_{i,s}1_{i,B}\varepsilon_{i,s}\\ \frac{1}{\sqrt{n}}\sum_{i\in N}\tilde{Z}_{i,s}1_{i,F}\varepsilon_{i,s}\end{bmatrix}=\sum_{s=1}^{T}\begin{bmatrix}\frac{1}{\sqrt{n_{B}}}\sum_{i\in N_{B}}\tilde{Z}_{i,s}\varepsilon_{i,s}\\ \frac{1}{\sqrt{n_{F}}}\sum_{i\in N_{F}}\tilde{Z}_{i,s}\varepsilon_{i,s}\end{bmatrix}=\begin{bmatrix}\sqrt{n_{B}}\hat{U}_{B}\\ \sqrt{n_{F}}\hat{U}_{F}\end{bmatrix}.$$

Hence

$$\begin{bmatrix}\sqrt{n_{B}}\hat{V}_{B}^{-1/2}(\hat{\delta}_{B}-\delta_{B})\\ \sqrt{n_{F}}\hat{V}_{F}^{-1/2}(\hat{\delta}_{F}-\delta_{F})\end{bmatrix}=\begin{bmatrix}\left(\hat{B}_{B}^{\top}\hat{\Omega}_{B}^{-1}\hat{B}_{B}\right)^{-1/2}\hat{B}_{B}^{\top}\hat{\Omega}_{B}^{-1} & 0\\ 0 & \left(\hat{B}_{F}^{\top}\hat{\Omega}_{F}^{-1}\hat{B}_{F}\right)^{-1/2}\hat{B}_{F}^{\top}\hat{\Omega}_{F}^{-1}\end{bmatrix}\sqrt{n}\hat{U}. \tag{1.10}$$

By Lemma 1.8 and Cramér-Wold device, we find that

$$\Omega^{-1/2}\sqrt{n}\hat{U}\rightarrow_{d}N(0,I),$$

as $n \to \infty$. This implies that $\sqrt{n}\hat{U} = O_P(1)$.

Since $\sqrt{n}\hat{U} = O_P(1)$, the last term in (1.10) is written as

$$\begin{bmatrix} \left(B_B^\top \Omega_B^{-1} B_B\right)^{-1/2} B_B^\top \Omega_B^{-1} & 0 \\ 0 & \left(B_F^\top \Omega_F^{-1} B_F\right)^{-1/2} B_F^\top \Omega_F^{-1} \end{bmatrix} \sqrt{n}\hat{U} + o_P(1)$$

$$= \begin{bmatrix} \left(B_B^\top \Omega_B^{-1} B_B\right)^{-1/2} B_B^\top \Omega_B^{-1/2} & 0 \\ 0 & \left(B_F^\top \Omega_F^{-1} B_F\right)^{-1/2} B_F^\top \Omega_F^{-1/2} \end{bmatrix} \Omega^{-1/2}\sqrt{n}\hat{U} + o_P(1).$$

The leading term on the right hand side converges in distribution to $N(0, I)$, which is our desired result. ■

Proof of Theorem 3.2: In view of Theorem 2.1 of Romano and Shaikh (2010), it suffices to show the following three statements:

(a) $\lim_{n\to\infty} P\left\{\hat{Q}_{FB} \leq c_{1-\alpha}\right\} = 1-\alpha$.
(b) $\lim_{n\to\infty} P\left\{\hat{Q}_{BF} \leq c_{1-\alpha}\right\} = 1-\alpha$.
(c) $\lim_{n\to\infty} P\left\{\max\{\hat{Q}_{FB}, \hat{Q}_{BF}\} \leq c_{\sqrt{1-\alpha}}\right\} = 1-\alpha$.

The statements (a) and (b) follow from Theorem 3.1 immediately by the Continuous Mapping Theorem (CMT). We show (c). Again, by the CMT applied to Theorem 3.1, we find that as $n \to \infty$, $\left[\hat{Q}_{FB}, \hat{Q}_{BF}\right]^\top \to_d [Q_1, Q_2]^\top$, where Q_1 and Q_2 are independent random variables that follow $\chi^2(1)$. Since the maximum is a continuous map, by the CMT, we have as $n \to \infty$,

$$\begin{aligned} P\left\{\max\{\hat{Q}_{FB}, \hat{Q}_{BF}\} \leq c_{\sqrt{1-\alpha}}\right\} &= P\left\{\max\{Q_1, Q_2\} \leq c_{\sqrt{1-\alpha}}\right\} + o(1) \\ &= P\left\{Q_1 \leq c_{\sqrt{1-\alpha}}\right\} P\left\{Q_2 \leq c_{\sqrt{1-\alpha}}\right\} + o(1) \\ &= \left(\sqrt{1-\alpha}\right)^2 + o(1) = 1-\alpha+o(1). \end{aligned}$$

Thus, we have the desired result. ■

2. Further Results from the Monte Carlo Simulation Study

We present further results from our Monte Carlo study based on using alternative choices of instruments. We investigate the size and power properties of each case. For instruments, we consider three alternatives: the IVs based on the LP with option A, the IVs based on LP with option C, and the IV's based on Hayakawa's Backward Orthogonal Deviation. In exploring these results, we use the same networks as used in the main text.

The results are reported in Tables 9-17. The empirical sizes are shown in Tables 9-11. As we can see, the sizes are quite stable across all specifications of instruments and networks

TABLE 9. Empirical Rejection Probabilities under the Null Hypothesis (with IVs based on the LP with option A)

$\bar{\beta}_{FB} = 0$, $\alpha_B = \alpha_F = 0$, and $\beta_{BF} = \beta_{BB} = \beta_{FF} = 0$

		BA 1		BA 5		BA 9	
n	α	$T=5$	$T=10$	$T=5$	$T=10$	$T=5$	$T=10$
500	0.01	0.014	0.018	0.012	0.014	0.015	0.014
	0.05	0.065	0.070	0.062	0.061	0.063	0.063
	0.10	0.119	0.127	0.12	0.114	0.124	0.122
5000	0.01	0.009	0.010	0.010	0.008	0.009	0.011
	0.05	0.053	0.057	0.050	0.047	0.054	0.050
	0.10	0.102	0.105	0.100	0.097	0.103	0.102

$\bar{\beta}_{FB} = 1$, $\alpha_B = \alpha_F = 1$, and $\beta_{BF} = \beta_{BB} = \beta_{FF} = 1$

		BA 1		BA 5		BA 9	
n	α	$T=5$	$T=10$	$T=5$	$T=10$	$T=5$	$T=10$
500	0.01	0.014	0.014	0.010	0.017	0.009	0.015
	0.05	0.063	0.065	0.054	0.069	0.056	0.065
	0.10	0.116	0.124	0.108	0.132	0.114	0.113
5000	0.01	0.009	0.012	0.009	0.012	0.01	0.011
	0.05	0.051	0.057	0.048	0.052	0.051	0.053
	0.10	0.103	0.115	0.099	0.104	0.096	0.110

$\bar{\beta}_{FB} = 1$, $\bar{\beta}_{BF} = 0$, with $\alpha_B = \alpha_F = 1$, and $\beta_{BB} = \beta_{FF} = 0$

		BA 1		BA 5		BA 9	
n	α	$T=5$	$T=10$	$T=5$	$T=10$	$T=5$	$T=10$
500	0.01	0.008	0.011	0.008	0.011	0.012	0.015
	0.05	0.053	0.060	0.048	0.058	0.057	0.065
	0.10	0.114	0.111	0.103	0.116	0.118	0.120
5000	0.01	0.009	0.008	0.009	0.011	0.011	0.011
	0.05	0.042	0.043	0.047	0.057	0.057	0.053
	0.10	0.088	0.091	0.096	0.107	0.107	0.101

Notes: The table presents the empirical rejection probability under the null hypothesis that $\beta_{FB} = \bar{\beta}_{FB}$, where we choose $\bar{\beta}_{FB} = 0$ or $\bar{\beta}_{FB} = 1$. As before, the "BA-1", "BA-2" and "BA-3" represent the graphs generated according to Barabási-Albert graphs with varied denseness. The numbers $\alpha = 0.01, 0.05, 0.10$ denote the nominal level of the test used in this study. The Monte Carlo simulation number was 5,000.

considered here. There is no size distortion as the network gets denser. The empirical powers are reported in Tables 12-14. The empirical power from using the IVs based on the LP with option C appears slightly higher than option A. Surprisingly the empirical power based on the IVs using the Backward Orthogonal Deviation is low in our setting. Finally, we look into empirical Familywise Error Rate. The results are reported in Tables 15-17. The results look quite reasonable across all specifications of instruments and networks considered here, without much noticeable differences.

TABLE 10. Empirical Rejection Probabilities under the Null Hypothesis (with IVs based on the LP with option C)

$\bar{\beta}_{FB} = 0$, $\alpha_B = \alpha_F = 0$, and $\beta_{BF} = \beta_{BB} = \beta_{FF} = 0$

		BA 1		BA 5		BA 9	
n	α	$T=5$	$T=10$	$T=5$	$T=10$	$T=5$	$T=10$
500	0.01	0.013	0.016	0.013	0.013	0.016	0.015
	0.05	0.068	0.063	0.065	0.059	0.066	0.066
	0.10	0.127	0.122	0.120	0.110	0.124	0.125
5000	0.01	0.012	0.011	0.01	0.011	0.011	0.008
	0.05	0.053	0.050	0.055	0.050	0.049	0.049
	0.10	0.108	0.100	0.111	0.101	0.096	0.098

$\bar{\beta}_{FB} = 1$, $\alpha_B = \alpha_F = 1$, and $\beta_{BF} = \beta_{BB} = \beta_{FF} = 1$

		BA 1		BA 5		BA 9	
n	α	$T=5$	$T=10$	$T=5$	$T=10$	$T=5$	$T=10$
500	0.01	0.013	0.012	0.013	0.014	0.018	0.015
	0.05	0.059	0.058	0.068	0.070	0.076	0.067
	0.10	0.119	0.118	0.134	0.126	0.141	0.121
5000	0.01	0.010	0.011	0.012	0.010	0.014	0.009
	0.05	0.049	0.051	0.056	0.050	0.059	0.052
	0.10	0.108	0.103	0.107	0.098	0.109	0.102

$\bar{\beta}_{FB} = 1$, $\bar{\beta}_{BF} = 0$, with $\alpha_B = \alpha_F = 1$, and $\beta_{BB} = \beta_{FF} = 0$

		BA 1		BA 5		BA 9	
n	α	$T=5$	$T=10$	$T=5$	$T=10$	$T=5$	$T=10$
500	0.01	0.015	0.018	0.019	0.019	0.021	0.022
	0.05	0.068	0.067	0.078	0.076	0.091	0.079
	0.10	0.127	0.134	0.144	0.136	0.157	0.142
5000	0.01	0.008	0.009	0.012	0.013	0.012	0.013
	0.05	0.049	0.050	0.056	0.057	0.063	0.053
	0.10	0.103	0.110	0.105	0.109	0.111	0.107

Notes: The table presents the empirical rejection probability under the null hypothesis that $\beta_{FB} = \bar{\beta}_{FB}$, where we choose $\bar{\beta}_{FB} = 0$ or $\bar{\beta}_{FB} = 1$. As before, the "BA-1", "BA-2" and "BA-3" represent the graphs generated according to Barabási-Albert graphs with varied denseness. The numbers $\alpha = 0.01, 0.05, 0.10$ denote the nominal level of the test used in this study. The Monte Carlo simulation number was 5,000.

TABLE 11. Empirical Rejection Probabilities under the Null Hypothesis (with IVs based on the Backward Orthogonal Deviation)

$\bar{\beta}_{FB} = 0$, $\alpha_B = \alpha_F = 0$, and $\beta_{BF} = \beta_{BB} = \beta_{FF} = 0$

		BA 1		BA 5		BA 9	
n	α	$T=5$	$T=10$	$T=5$	$T=10$	$T=5$	$T=10$
500	0.01	0.018	0.012	0.013	0.014	0.014	0.014
	0.05	0.072	0.061	0.063	0.064	0.060	0.058
	0.10	0.129	0.119	0.116	0.123	0.120	0.112
5000	0.01	0.011	0.011	0.013	0.011	0.010	0.008
	0.05	0.047	0.044	0.047	0.049	0.047	0.049
	0.10	0.097	0.096	0.095	0.102	0.097	0.104

$\bar{\beta}_{FB} = 1$, $\alpha_B = \alpha_F = 1$, and $\beta_{BF} = \beta_{BB} = \beta_{FF} = 1$

		BA 1		BA 5		BA 9	
n	α	$T=5$	$T=10$	$T=5$	$T=10$	$T=5$	$T=10$
500	0.01	0.014	0.016	0.010	0.018	0.007	0.014
	0.05	0.058	0.066	0.052	0.063	0.045	0.063
	0.10	0.114	0.124	0.107	0.128	0.095	0.119
5000	0.01	0.010	0.009	0.008	0.008	0.013	0.013
	0.05	0.055	0.052	0.046	0.050	0.053	0.051
	0.10	0.113	0.103	0.095	0.098	0.106	0.100

$\bar{\beta}_{FB} = 1$, $\bar{\beta}_{BF} = 0$, with $\alpha_B = \alpha_F = 1$, and $\beta_{BB} = \beta_{FF} = 0$

		BA 1		BA 5		BA 9	
n	α	$T=5$	$T=10$	$T=5$	$T=10$	$T=5$	$T=10$
500	0.01	0.000	0.001	0.001	0.004	0.003	0.005
	0.05	0.008	0.015	0.014	0.036	0.028	0.041
	0.10	0.027	0.043	0.047	0.094	0.062	0.097
5000	0.01	0.001	0.006	0.007	0.008	0.009	0.011
	0.05	0.014	0.038	0.045	0.045	0.05	0.052
	0.10	0.045	0.084	0.099	0.095	0.100	0.104

Notes: The table presents the empirical rejection probability under the null hypothesis that $\beta_{FB} = \bar{\beta}_{FB}$, where we choose $\bar{\beta}_{FB} = 0$ or $\bar{\beta}_{FB} = 1$. As before, the "BA-1", "BA-2" and "BA-3" represent the graphs generated according to Barabási-Albert graphs with varied denseness. The numbers $\alpha = 0.01, 0.05, 0.10$ denote the nominal level of the test used in this study. The Monte Carlo simulation number was 5,000.

TABLE 12. Empirical Rejection Probabilities under the Alternative Hypothesis: $\beta_{FB} = \bar{\beta}_{FB} + \Delta$ at the Nominal Level 0.05 (with IVs based on the LP with option A)

$\bar{\beta}_{FB} = 0$, $\alpha_B = \alpha_F = 0$, and $\beta_{BF} = \beta_{BB} = \beta_{FF} = 0$

		BA 1		BA 5		BA 9	
n	Δ	$T=5$	$T=10$	$T=5$	$T=10$	$T=5$	$T=10$
500	0.10	0.999	1.000	0.642	0.957	0.425	0.778
	0.5	1.000	1.000	1.000	1.000	1.000	1.000
5000	0.10	1.000	1.000	1.000	1.000	1.000	1.000
	0.5	1.000	1.000	1.000	1.000	1.000	1.000

$\bar{\beta}_{FB} = 1$, $\alpha_B = \alpha_F = 1$, and $\beta_{BF} = \beta_{BB} = \beta_{FF} = 1$

		BA 1		BA 5		BA 9	
n	Δ	$T=5$	$T=10$	$T=5$	$T=10$	$T=5$	$T=10$
500	0.10	1.000	1.000	0.258	1.000	0.111	0.992
	0.5	1.000	1.000	0.999	1.000	0.935	1.000
5000	0.10	1.000	1.000	0.991	1.000	0.697	1.000
	0.5	1.000	1.000	1.000	1.000	1.000	1.000

$\bar{\beta}_{FB} = 1$, $\bar{\beta}_{BF} = 0$, with $\alpha_B = \alpha_F = 1$, and $\beta_{BB} = \beta_{FF} = 0$

		BA 1		BA 5		BA 9	
n	Δ	$T=5$	$T=10$	$T=5$	$T=10$	$T=5$	$T=10$
500	0.10	0.200	0.761	0.065	0.323	0.064	0.251
	0.5	0.990	1.000	0.794	1.000	0.718	0.999
5000	0.10	0.556	1.000	0.38	0.991	0.339	0.983
	0.5	1.000	1.000	1.000	1.000	1.000	1.000

Notes: The table shows the empirical rejection probability under the alternative hypothesis that $\beta_{FB} = \bar{\beta}_{FB} + \Delta$ at the nominal level 0.05, where we choose $\bar{\beta}_{FB} = 0$ or $\bar{\beta}_{FB} = 1$, and $\Delta \in \{0.1, 0.5\}$. As before, the "BA-1", "BA-2" and "BA-3" represent the graphs generated according to Erdös-Rényi graphs with different configurations of the denseness of the networks. The Monte Carlo simulation number was 5,000. As expected, the power of the test increases with the sample size. It is also worth noting that it also increases substantially as the time T increases from $T = 5$ to $T = 10$. Most importantly, as the network becomes denser, the power decreases.

TABLE 13. Empirical Rejection Probabilities under the Alternative Hypothesis: $\beta_{FB} = \bar{\beta}_{FB} + \Delta$ at the Nominal Level 0.05 (with IVs based on the LP with option C)

$\bar{\beta}_{FB} = 0$, $\alpha_B = \alpha_F = 0$, and $\beta_{BF} = \beta_{BB} = \beta_{FF} = 0$

		BA 1		BA 5		BA 9	
n	Δ	$T=5$	$T=10$	$T=5$	$T=10$	$T=5$	$T=10$
500	0.10	1.000	1.000	0.646	0.963	0.428	0.790
	0.5	1.000	1.000	1.000	1.000	1.000	1.000
5000	0.10	1.000	1.000	1.000	1.000	1.000	1.000
	0.5	1.000	1.000	1.000	1.000	1.000	1.000

$\bar{\beta}_{FB} = 1$, $\alpha_B = \alpha_F = 1$, and $\beta_{BF} = \beta_{BB} = \beta_{FF} = 1$

		BA 1		BA 5		BA 9	
n	Δ	$T=5$	$T=10$	$T=5$	$T=10$	$T=5$	$T=10$
500	0.10	1.000	1.000	0.296	1.000	0.11	0.997
	0.5	1.000	1.000	1.000	1.000	0.982	1.000
5000	0.10	1.000	1.000	0.989	1.000	0.716	1.000
	0.5	1.000	1.000	1.000	1.000	1.000	1.000

$\bar{\beta}_{FB} = 1$, $\bar{\beta}_{BF} = 0$, with $\alpha_B = \alpha_F = 1$, and $\beta_{BB} = \beta_{FF} = 0$

		BA 1		BA 5		BA 9	
n	Δ	$T=5$	$T=10$	$T=5$	$T=10$	$T=5$	$T=10$
500	0.10	0.372	0.955	0.074	0.367	0.068	0.268
	0.5	1.000	1.000	0.930	1.000	0.85	1.000
5000	0.10	0.718	1.000	0.369	0.991	0.311	0.981
	0.5	1.000	1.000	1.000	1.000	1.000	1.000

Notes: The table shows the empirical rejection probability under the alternative hypothesis that $\beta_{FB} = \bar{\beta}_{FB} + \Delta$ at the nominal level 0.05, where we choose $\bar{\beta}_{FB} = 0$ or $\bar{\beta}_{FB} = 1$, and $\Delta \in \{0.1, 0.5\}$. As before, the "BA-1", "BA-2" and "BA-3" represent the graphs generated according to Erdös-Rényi graphs with different configurations of the denseness of the networks. The Monte Carlo simulation number was 5,000. As expected, the power of the test increases with the sample size. It is also worth noting that it also increases substantially as the time T increases from $T = 5$ to $T = 10$. Most importantly, as the network becomes denser, the power decreases.

TABLE 14. Empirical Rejection Probabilities under the Alternative Hypothesis: $\beta_{FB} = \bar{\beta}_{FB} + \Delta$ at the Nominal Level 0.05 (with IVs based on the Backward Orthogonal Deviation)

$\bar{\beta}_{FB} = 0$, $\alpha_B = \alpha_F = 0$, and $\beta_{BF} = \beta_{BB} = \beta_{FF} = 0$

		BA 1		BA 5		BA 9	
n	Δ	$T=5$	$T=10$	$T=5$	$T=10$	$T=5$	$T=10$
500	0.10	0.960	1.000	0.393	0.913	0.271	0.708
	0.5	1.000	1.000	1.000	1.000	1.000	1.000
5000	0.10	1.000	1.000	1.000	1.000	0.992	1.000
	0.5	1.000	1.000	1.000	1.000	1.000	1.000

$\bar{\beta}_{FB} = 1$, $\alpha_B = \alpha_F = 1$, and $\beta_{BF} = \beta_{BB} = \beta_{FF} = 1$

		BA 1		BA 5		BA 9	
n	Δ	$T=5$	$T=10$	$T=5$	$T=10$	$T=5$	$T=10$
500	0.10	1.000	1.000	0.226	1.000	0.090	0.986
	0.5	1.000	1.000	0.995	1.000	0.821	1.000
5000	0.10	1.000	1.000	0.990	1.000	0.625	1.000
	0.5	1.000	1.000	1.000	1.000	1.000	1.000

$\bar{\beta}_{FB} = 1$, $\bar{\beta}_{BF} = 0$, with $\alpha_B = \alpha_F = 1$, and $\beta_{BB} = \beta_{FF} = 0$

		BA 1		BA 5		BA 9	
n	Δ	$T=5$	$T=10$	$T=5$	$T=10$	$T=5$	$T=10$
500	0.10	0.029	0.115	0.019	0.095	0.027	0.096
	0.5	0.344	0.619	0.214	0.783	0.220	0.820
5000	0.10	0.082	0.517	0.120	0.512	0.121	0.526
	0.5	0.653	0.983	0.947	1.000	0.959	1.000

Notes: The table shows the empirical rejection probability under the alternative hypothesis that $\beta_{FB} = \bar{\beta}_{FB} + \Delta$ at the nominal level 0.05, where we choose $\bar{\beta}_{FB} = 0$ or $\bar{\beta}_{FB} = 1$, and $\Delta \in \{0.1, 0.5\}$. As before, the "BA-1", "BA-2" and "BA-3" represent the graphs generated according to Erdös-Rényi graphs with different configurations of the denseness of the networks. The Monte Carlo simulation number was 5,000. As expected, the power of the test increases with the sample size. It is also worth noting that it also increases substantially as the time T increases from $T = 5$ to $T = 10$. Most importantly, as the network becomes denser, the power decreases.

TABLE 15. Empirical Familywise Error Rate (with IVs based on the LP with option A)

$\bar{\beta}_{FB} = 0$, $\bar{\beta}_{BF} = 0$, with $\alpha_B = \alpha_F = 0$, and $\beta_{BB} = \beta_{FF} = 0$

		BA 1		BA 5		BA 9	
n	α	$T=5$	$T=10$	$T=5$	$T=10$	$T=5$	$T=10$
500	0.01	0.018	0.020	0.013	0.013	0.016	0.014
	0.05	0.067	0.074	0.064	0.064	0.066	0.069
	0.10	0.125	0.135	0.125	0.121	0.123	0.125
5000	0.01	0.009	0.009	0.010	0.010	0.007	0.010
	0.05	0.049	0.049	0.052	0.051	0.049	0.049
	0.10	0.106	0.105	0.100	0.100	0.106	0.099

$\bar{\beta}_{FB} = 1$, $\bar{\beta}_{BF} = 0$, with $\alpha_B = \alpha_F = 1$, and $\beta_{BB} = \beta_{FF} = 0$

		BA 1		BA 5		BA 9	
n	α	$T=5$	$T=10$	$T=5$	$T=10$	$T=5$	$T=10$
500	0.01	0.013	0.016	0.013	0.019	0.013	0.015
	0.05	0.053	0.067	0.059	0.071	0.059	0.064
	0.10	0.115	0.127	0.111	0.121	0.114	0.135
5000	0.01	0.012	0.009	0.013	0.011	0.010	0.011
	0.05	0.055	0.044	0.055	0.051	0.049	0.055
	0.10	0.105	0.096	0.109	0.104	0.103	0.108

Notes: The table presents the empirical Familywise Error Rate (FWER) for the step down procedure explain in Section 3.3. The nominal FWER is given by $\alpha = 0.01, 0.05, 0.10$.

TABLE 16. Empirical Familywise Error Rate (with IVs based on the LP with option C)

$\bar{\beta}_{FB} = 0$, $\bar{\beta}_{BF} = 0$, with $\alpha_B = \alpha_F = 0$, and $\beta_{BB} = \beta_{FF} = 0$

		BA 1		BA 5		BA 9	
n	α	$T=5$	$T=10$	$T=5$	$T=10$	$T=5$	$T=10$
500	0.01	0.018	0.017	0.018	0.015	0.017	0.015
	0.05	0.075	0.063	0.070	0.066	0.071	0.067
	0.10	0.135	0.122	0.128	0.123	0.122	0.131
5000	0.01	0.012	0.009	0.009	0.012	0.012	0.009
	0.05	0.050	0.055	0.053	0.051	0.047	0.049
	0.10	0.106	0.104	0.109	0.101	0.096	0.103

$\bar{\beta}_{FB} = 1$, $\bar{\beta}_{BF} = 0$, with $\alpha_B = \alpha_F = 1$, and $\beta_{BB} = \beta_{FF} = 0$

		BA 1		BA 5		BA 9	
n	α	$T=5$	$T=10$	$T=5$	$T=10$	$T=5$	$T=10$
500	0.01	0.015	0.015	0.013	0.014	0.013	0.015
	0.05	0.067	0.069	0.056	0.066	0.058	0.061
	0.10	0.130	0.130	0.116	0.121	0.111	0.116
5000	0.01	0.012	0.008	0.010	0.010	0.011	0.011
	0.05	0.055	0.052	0.049	0.047	0.050	0.052
	0.10	0.102	0.103	0.094	0.094	0.094	0.096

Notes: The table presents the empirical Familywise Error Rate (FWER) for the step down procedure explain in Section 3.3. The nominal FWER is given by $\alpha = 0.01, 0.05, 0.10$.

TABLE 17. Empirical Familywise Error Rate (with IVs based on the Backward Orthogonal Deviation)

$\bar{\beta}_{FB} = 0$, $\bar{\beta}_{BF} = 0$, with $\alpha_B = \alpha_F = 0$, and $\beta_{BB} = \beta_{FF} = 0$

		BA 1		BA 5		BA 9	
n	α	$T = 5$	$T = 10$	$T = 5$	$T = 10$	$T = 5$	$T = 10$
500	0.01	0.019	0.013	0.016	0.016	0.017	0.017
	0.05	0.070	0.064	0.064	0.071	0.066	0.067
	0.10	0.132	0.119	0.130	0.128	0.123	0.124
5000	0.01	0.010	0.012	0.010	0.012	0.009	0.009
	0.05	0.049	0.050	0.050	0.048	0.047	0.048
	0.10	0.096	0.095	0.097	0.097	0.099	0.100

$\bar{\beta}_{FB} = 1$, $\bar{\beta}_{BF} = 0$, with $\alpha_B = \alpha_F = 1$, and $\beta_{BB} = \beta_{FF} = 0$

		BA 1		BA 5		BA 9	
n	α	$T = 5$	$T = 10$	$T = 5$	$T = 10$	$T = 5$	$T = 10$
500	0.01	0.009	0.017	0.008	0.013	0.009	0.018
	0.05	0.046	0.062	0.046	0.062	0.046	0.072
	0.10	0.091	0.111	0.093	0.121	0.093	0.132
5000	0.01	0.010	0.010	0.010	0.012	0.011	0.011
	0.05	0.050	0.054	0.050	0.055	0.055	0.056
	0.10	0.100	0.100	0.099	0.097	0.106	0.106

Notes: The table presents the empirical Familywise Error Rate (FWER) for the step down procedure explain in Section 3.3. The nominal FWER is given by $\alpha = 0.01, 0.05, 0.10$.

3. Further Results from the Empirical Application

Here we report results cited from Section 4.6 which discusses robustness of our results. In Figures 3 and 4, we present the network characteristics based on the 10-th percentile thresholds and the 50-th percentile thresholds. Figure 5 presents the characteristics of the networks based on the debt share of firms in the sectors.

The estimation results are presented in Tables 18-23. We refer the reader to Section 4.6 for the discussion of these additional results.

FIGURE 3. Network characteristics (10th prc.)

(A) Sector to bank

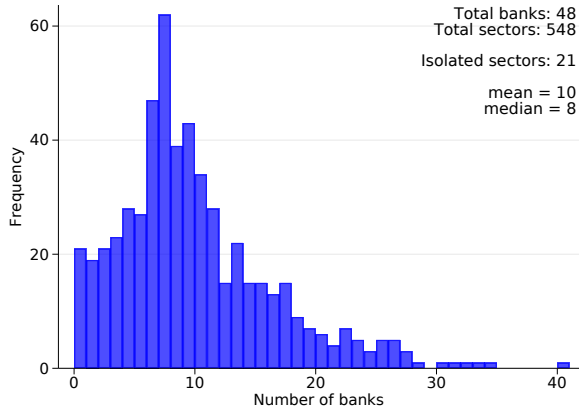

(B) Bank to sector

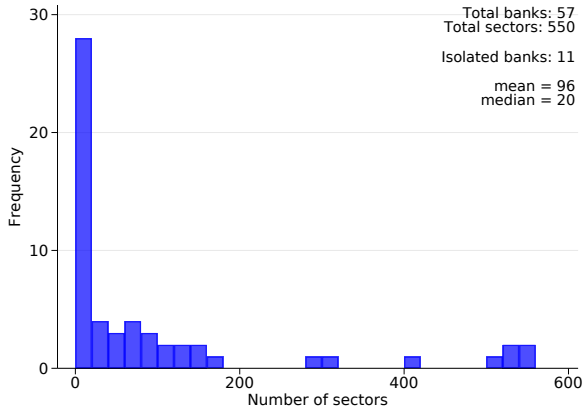

Notes: This figure shows the network characteristics for the baseline specification. Panel (a) shows the distribution of the number of sectors per bank, while Panel (b) shows the distribution of the number of banks per sector. The network thresholds in Panels (a) and (b) are set to the 10th percentile of the relevant debt share and asset share, respectively.

FIGURE 4. Network characteristics (50th prc.)

(A) Sector to bank

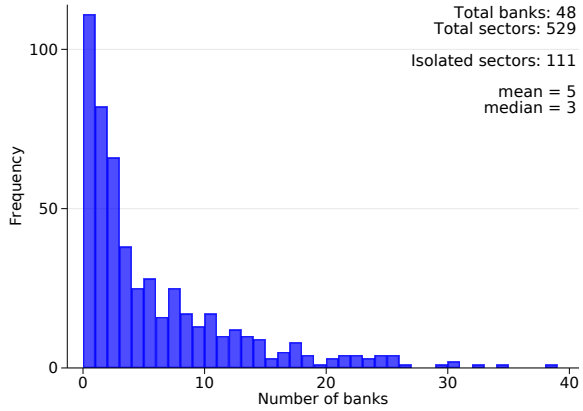

(B) Bank to sector

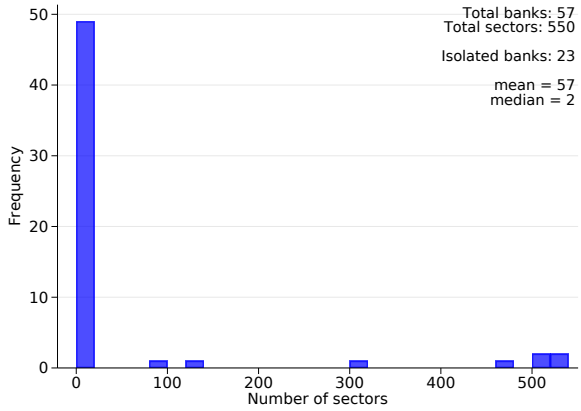

Notes: This figure shows the network characteristics for the baseline specification. Panel (a) shows the distribution of the number of sectors per bank, while Panel (b) shows the distribution of the number of banks per sector. The network thresholds in Panels (a) and (b) are set to the 50th percentile of the relevant debt share and asset share, respectively.

FIGURE 5. Network characteristics (25th prc.)

(A) Sector to bank

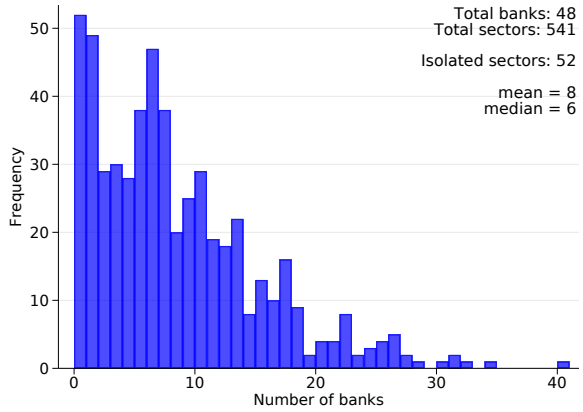

(B) Bank to sector

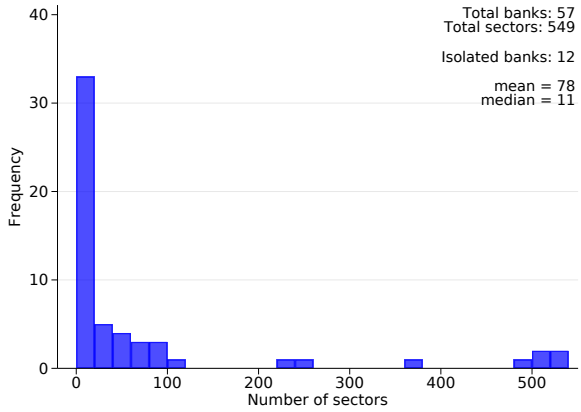

Notes: This figure shows the network characteristics for the baseline specification. Panel (a) shows the distribution of the number of sectors per bank, while Panel (b) shows the distribution of the number of banks per sector. The network thresholds in Panels (a) and (b) are set to the 25th percentile of the relevant debt share.

TABLE 18. Robustness: Sparser network (using IV based on LP with option B)

	Coef.	Std. err.	p-value	[95% Conf.	interval]
Panel A: Sector to bank					
Bank weakness $_{t-1}$	0.333	0.002	0.000	0.329	0.338
Zombie congestion $_{t-1}$	0.963	0.290	0.001	0.395	1.531
Number of banks	48				
Number of sectors	529				
Observations	23 616				
Panel B: Bank to sector					
Zombie congestion $_{t-1}$	0.695	0.049	0.000	0.599	0.791
Bank weakness $_{t-1}$	0.607	3.485	0.862	−6.224	7.438
Market concentration $_{t-1}$	−0.033	0.097	0.737	−0.224	0.158
Sales growth $_{t-1}$	0.000	0.008	0.951	−0.016	0.015
Capital intensity $_{t-1}$	−0.011	0.007	0.134	−0.024	0.003
Number of banks	57				
Number of sectors	550				
Observations	26 176				
Direction of spillover with FWER control	$S \to B$	at 1%			

Notes: This table shows the results from estimating equation (2.8). Panel A refers to the direction from sectors to banks while Panel B refers to the direction from banks to sectors. The network thresholds in Panels A and B are set to the 50th percentile of the relevant debt share and asset share, respectively. The sample contains all reported firm-bank relationships and covers the period between 2005 and 2012. Results are obtained using option B. Bank weakness is given by the ratio of loan loss provsions to total assets; zombie congestion is the asset-weighted share of zombie firms in a sector according to the baseline definition; market concentration is the HHI index of sector-level sales; sales growth is computed as the log difference in total sector sales from the year before; capital intensity is the share of a sector's fixed assets in total sales.

TABLE 19. Robustness: Denser network (using IV based on LP with option B)

	Coef.	Std. err.	p-value	[95% Conf.	interval]
Panel A: Sector to bank					
Bank weakness $_{t-1}$	0.330	0.002	0.000	0.326	0.334
Zombie congestion $_{t-1}$	0.920	0.298	0.002	0.335	1.505
Number of banks	48				
Number of sectors	548				
Observations	41 840				
Panel B: Bank to sector					
Zombie congestion $_{t-1}$	0.696	0.048	0.000	0.601	0.791
Bank weakness $_{t-1}$	0.150	0.056	0.007	0.041	0.260
Market concentration $_{t-1}$	−0.027	0.099	0.786	−0.220	0.167
Sales growth $_{t-1}$	−0.001	0.008	0.908	−0.016	0.014
Capital intensity $_{t-1}$	−0.014	0.009	0.091	−0.031	0.002
Number of banks	57				
Number of sectors	550				
Observations	43 936				
Direction of spillover with FWER control	$S \longleftrightarrow B$	at 1%			

Notes: This table shows the results from estimating equation (2.8). Panel A refers to the direction from sectors to banks while Panel B refers to the direction from banks to sectors. The network thresholds in Panels A and B are set to the 10th percentile of the relevant debt share and asset share, respectively. The sample contains all reported firm-bank relationships and covers the period between 2005 and 2012. Results are obtained using option B. Bank weakness is given by the ratio of loan loss provsions to total assets; zombie congestion is the asset-weighted share of zombie firms in a sector according to the baseline definition; market concentration is the HHI index of sector-level sales; sales growth is computed as the log difference in total sector sales from the year before; capital intensity is the share of a sector's fixed assets in total sales.

TABLE 20. Robustness: Networks based on debt only (using IV based on LP with option B)

	Coef.	Std. err.	p-value	[95% Conf.	interval]
Panel A: Sector to bank					
Bank weakness $_{t-1}$	0.330	0.002	0.000	0.326	0.334
Zombie congestion $_{t-1}$	0.964	0.322	0.003	0.333	1.596
Number of banks	48				
Number of sectors	541				
Observations	35 144				
Panel B: Bank to sector					
Zombie congestion $_{t-1}$	0.695	0.049	0.000	0.599	0.791
Bank weakness $_{t-1}$	0.140	0.096	0.146	−0.049	0.328
Market concentration $_{t-1}$	−0.028	0.099	0.777	−0.221	0.165
Sales growth $_{t-1}$	−0.001	0.008	0.898	−0.016	0.014
Capital intensity $_{t-1}$	−0.015	0.009	0.090	−0.032	0.002
Number of banks	57				
Number of sectors	549				
Observations	35 680				
Direction of spillover with FWER control	$S \to B$	at 1%			

Notes: This table shows the results from estimating equation (2.8). Panel A refers to the direction from sectors to banks while Panel B refers to the direction from banks to sectors. The network thresholds in Panels A and B are set to the 25th percentile of the relevant debt share. The sample contains all reported firm-bank relationships and covers the period between 2005 and 2012. Results are obtained using option B. Bank weakness is given by the ratio of loan loss provsions to total assets; zombie congestion is the asset-weighted share of zombie firms in a sector according to the baseline definition; market concentration is the HHI index of sector-level sales; sales growth is computed as the log difference in total sector sales from the year before; capital intensity is the share of a sector's fixed assets in total sales.

TABLE 21. Robustness: First bank only (using IV based on LP with option B)

	Coef.	Std. err.	p-value	[95% Conf.	interval]
Panel A: Sector to bank					
Bank weakness $_{t-1}$	0.335	0.002	0.000	0.331	0.339
Zombie congestion $_{t-1}$	0.751	0.519	0.148	−0.266	1.769
Number of banks	46				
Number of sectors	537				
Observations	26 552				
Panel B: Bank to sector					
Zombie congestion $_{t-1}$	0.696	0.049	0.000	0.601	0.792
Bank weakness $_{t-1}$	0.133	0.040	0.001	0.053	0.212
Market concentration $_{t-1}$	−0.027	0.098	0.784	−0.219	0.166
Sales growth $_{t-1}$	−0.001	0.008	0.914	−0.016	0.014
Capital intensity $_{t-1}$	−0.015	0.009	0.090	−0.032	0.002
Number of banks	57				
Number of sectors	550				
Observations	28 512				
Direction of spillover with FWER control	$B \to S$	at 1%			

Notes: This table shows the results from estimating equation (2.8). Panel A refers to the direction from sectors to banks while Panel B refers to the direction from banks to sectors. The network thresholds in Panels A and B are set to the 25th percentile of the relevant debt share and asset share, respectively. The sample only includes the first reported bank relationship for each firm and covers the period between 2005 and 2012. Results are obtained using option B. Bank weakness is given by the ratio of loan loss provsions to total assets; zombie congestion is the asset-weighted share of zombie firms in a sector according to the baseline definition; market concentration is the HHI index of sector-level sales; sales growth is computed as the log difference in total sector sales from the year before; capital intensity is the share of a sector's fixed assets in total sales.

TABLE 22. Baseline specification (using IV based on LP with option A)

	Coef.	Std. err.	p-value	[95% Conf.	interval]
Panel A: Sector to bank					
Bank weakness $_{t-1}$	0.281	0.010	0.000	0.262	0.300
Zombie congestion $_{t-1}$	5.715	3.801	0.133	−1.734	13.164
Number of banks	48				
Number of sectors	541				
Observations	35 144				
Panel B: Bank to sector					
Zombie congestion $_{t-1}$	0.710	0.059	0.000	0.595	0.825
Bank weakness $_{t-1}$	0.147	0.050	0.003	0.050	0.245
Market concentration $_{t-1}$	−0.086	0.110	0.434	−0.302	0.130
Sales growth $_{t-1}$	0.001	0.008	0.890	−0.015	0.017
Capital intensity $_{t-1}$	−0.014	0.011	0.208	−0.037	0.008
Number of banks	57				
Number of sectors	550				
Observations	37 448				
Direction of spillover with FWER control	$B \to S$	at 1%			

Notes: This table shows the results from estimating equation (2.8). Panel A refers to the direction from sectors to banks while Panel B refers to the direction from banks to sectors. The network thresholds in Panels A and B are set to the 25th percentile of the relevant debt share and asset share, respectively. The sample contains all reported firm-bank relationships and covers the period between 2005 and 2012. Results are obtained using option A. Bank weakness is given by the ratio of loan loss provsions to total assets; zombie congestion is the asset-weighted share of zombie firms in a sector according to the baseline definition; market concentration is the HHI index of sector-level sales; sales growth is computed as the log difference in total sector sales from the year before; capital intensity is the share of a sector's fixed assets in total sales.

TABLE 23. Baseline specification (using IV based on LP with option C)

	Coef.	Std. err.	p-value	[95% Conf.	interval]
Panel A: Sector to bank					
Bank weakness $_{t-1}$	0.330	0.002	0.000	0.326	0.333
Zombie congestion $_{t-1}$	0.712	0.312	0.023	0.100	1.325
Number of banks	48				
Number of sectors	541				
Observations	35 144				
Panel B: Bank to sector					
Zombie congestion $_{t-1}$	0.688	0.050	0.000	0.589	0.787
Bank weakness $_{t-1}$	0.134	0.047	0.005	0.041	0.227
Market concentration $_{t-1}$	0.014	0.099	0.891	−0.181	0.208
Sales growth $_{t-1}$	−0.002	0.008	0.808	−0.018	0.014
Capital intensity $_{t-1}$	−0.007	0.005	0.136	−0.016	0.002
Number of banks	57				
Number of sectors	550				
Observations	37 448				
Direction of spillover with FWER control	$B \longleftrightarrow S$	at 1%			

Notes: This table shows the results from estimating equation (2.8). Panel A refers to the direction from sectors to banks while Panel B refers to the direction from banks to sectors. The network thresholds in Panels A and B are set to the 25th percentile of the relevant debt share and asset share, respectively. The sample contains all reported firm-bank relationships and covers the period between 2005 and 2012. Results are obtained using option C. Bank weakness is given by the ratio of loan loss provsions to total assets; zombie congestion is the asset-weighted share of zombie firms in a sector according to the baseline definition; market concentration is the HHI index of sector-level sales; sales growth is computed as the log difference in total sector sales from the year before; capital intensity is the share of a sector's fixed assets in total sales.